Electronic Thesis and Dissertation Repository

8-22-2018 9:30 AM

Elucidating the Importance of HopE and its Potential Lewis Glycosylation in *Helicobacter pylori*

Keertika Yogendirarajah, *The University of Western Ontario*

Supervisor: Creuzenet, Carole, *The University of Western Ontario*
A thesis submitted in partial fulfillment of the requirements for the Master of Science degree in Microbiology and Immunology
© Keertika Yogendirarajah 2018

Follow this and additional works at: https://ir.lib.uwo.ca/etd

🎨 Part of the Bacteria Commons, Bacterial Infections and Mycoses Commons, and the Digestive System Diseases Commons

Abstract

Helicobacter pylori colonizes 50% of the world's population, whereby glycoproteins and Lewis Y-containing lipopolysaccharides contribute to its pathogenesis. We investigated whether the HopE porin is glycosylated, if the glycan is Lewis Y, and if this is mediated by the putative oligosaccharide transferase HP0946 or the O-antigen ligase WaaL. Western blotting was performed on outer membranes with anti-HopE antibodies, anti-Lewis Y antibodies and fucose-binding BambL lectin to ascertain HopE glycosylation. We discovered that HopE is likely glycosylated by a non-Lewis Y fucose-containing glycan and neither HP0946 nor WaaL are the transferase. Additionally, we investigated HopE's role in antibiotic susceptibility via Etest strips and disk diffusion method. By comparing sets of mutants for HopE, HP0946, and WaaL, we found that HopE does not affect antibiotic sensitivity, while eliminating HP0946 increases antibiotic sensitivity. Overall, this study presents HopE as a novel fucosylated glycoprotein and introduces a possible role for HP0946 in antibiotic resistance.

Keywords

Acknowledgments

What a ride this was! To be honest this is the section of my thesis that intimidated me the most and given the fact that the whole thesis intimidated me, that's saying something.

To start, I would like to thank Western University and my supervisor Dr. Carole Creuzenet for giving me the opportunity to learn and grow here in London. Thank you Dr. Creuzenet for your continuous support and motivation, and for pushing me to constantly improve my skills. Aside from the technical, analytical thinking, and problem-solving skills that I learned from the Creuzenet lab, I also learned how to better handle setbacks and how even unexpected results can be helpful.

I would also like to thank my committee members, Dr. John McCormick and Dr. David Heinrichs for their support and helpful comments/suggestions regarding my project.

Continuing on, I want to thank all the members of the Creuzenet lab that I had the pleasure of working with and laughing with. You were all a great source of camaraderie and support. Special shout out to Dr. Najwa Zebian for helping me navigate the Creuzenet lab and always giving me a helping hand and answering my myriad of questions!

Penultimately, I give thanks to the friends I have made along my master's journey (#PromiscuousReceptors). Not only were you there to commiserate with me over the bad times but you also were there to celebrate the good times. Cheers to that.

Last but not least, I thank my mom and dad for their support in my academic choices and for shipments of home food. Your "starving" daughter appreciates every and any opportunity to skip cooking.

This couldn't have been done without you all.

Table of Contents

List of Tables

List of Figures

Chapter 1: Introduction

1   Introduction

1.1   An introduction to *Helicobacter pylori*

Helicobacter pylori is a Gram-negative, microaerophilic bacterium with a spiral shape and several polar sheathed flagella[1]. Currently, it is well known that *H. pylori* can survive the harsh environment of the human stomach and can cause gastritis, peptic ulcer disease[2] and gastric adenocarcinoma[1]. However, at the time of its discovery, the evidence that *H. pylori* could successfully colonize the stomach was controversial to the long-standing belief that stress and lifestyle were the major factors in the manifestation of peptic ulcer disease[3].

H. pylori was first isolated in 1982 by two Australian researchers, Barry Marshall and Robin Warren. Through drinking a culture of *H. pylori*, Dr. Marshall was able to demonstrate the association of *H. pylori* infection with gastritis and peptic ulcer disease when he developed gastritis after drinking the concoction[4]. Dr. Marshall's experiment was revolutionary as it followed Koch's postulates for the development of *H. pylori*-associated gastritis and proved that the stomach was not a sterile environment, incapable of bacterial colonization[4]. As a result of this significant finding and the subsequent association with gastric cancer, Dr. Marshall and Dr. Warren were awarded the Nobel Prize in Physiology and Medicine in 2005 for their discovery of *H. pylori*'s involvement in chronic gastrointestinal disease.

1.1.1   Clinical manifestation of *H. pylori*

Thirty-six years later, it is now recognized that *H. pylori* globally colonizes more than half of the world's population[5]. Although present throughout the world, there is a large geographic variation in *H. pylori*'s prevalence based on socioeconomic factors and levels of hygiene[6]. The countries with the highest prevalence are Nigeria (87.7%), Portugal (86.4%), and Estonia (82.5%) whereas the countries with the lowest prevalence are Switzerland (18.9%), Denmark (22.1%), and New Zealand (24.0%). While the United States has a low prevalence of *H. pylori* (35.6%), its indigenous populations have a high

prevalence (74.8%)[6]. According to the Canadian Digestive Health Foundation, 10 million (27.5%) Canadians are infected with *H. pylori*, with roughly 75% of the First Nation communities infected.

Helicobacter pylori is the only microorganism that can cause gastric adenocarcinoma, and it is the first pathogen to be classified as a type 1 human carcinogen by the World Health Organization (WHO)[5,7]. Although only 1-3% of infected individuals develop gastric cancer[8], this represents staggering numbers of affected individuals since *H. pylori* colonizes a large portion of the world's population. This contributes to gastric cancer being the 5th cancer worldwide for prevalence[9].

In order to treat *H. pylori* infections, suggested regimens include triple therapy or quadruple therapy[10]. Triple therapies involve the use of two antibiotics in combination with a proton pump inhibitor. However, due to the rise in antibiotic resistance, quadruple therapies are increasingly being prescribed. These therapies use a proton pump inhibitor, two antibiotics, a bismuth product and/or another antibiotic[11]. Proton pump inhibitors are used to suppress acid production and, in conjunction with the antibiotics, can help alleviate ulcer-related symptoms[11]. To date, antibiotic resistance and lack of patient tolerance has resulted in an increasing antibiotic treatment failure rate[12]. In fact, in 2017 the WHO published its first ever list of antibiotic-resistant "priority pathogens", a list of bacteria that pose the greatest threat to human health[13]. This list was created to guide and promote the research and development of new antibiotics for these priority pathogens. On the list, *Helicobacter pylori* was categorized as a "Priority 2: HIGH", for its increasing drug resistance to clarithromycin, which is used in first line therapies for the treatment of *H. pylori* infections. Thus, it is mandatory to find novel avenues of treatment for individuals suffering from diseases caused by chronic *H. pylori* infections.

1.2   The lipopolysaccharide (LPS)

The LPS layer is a key component of the outer membrane of *H. pylori*. The structure of *H. pylori*'s LPS is similar to the LPS of other Gram-negative bacteria and is composed of three domains: the hydrophobic lipid A domain embedded in the outer membrane, the core oligosaccharide, and the variable O-antigen polysaccharide[14] (Figure 1). This negatively charged structure plays a major role in providing a physical barrier against host defenses, detergents and antibiotics[15].

Each domain of the LPS has a unique function. Lipid A serves as the membrane anchoring component and is usually an endotoxin responsible for certain pathologies during infections. Specifically, toll-like receptor 4 (TLR4), a receptor protein on animal cells, is activated by lipid A, inducing the release of proinflammatory cytokines via signal transduction and triggering the innate immune response[16]. If the immune response is strong enough, this activation can result in sepsis, leading to organ failure and death[16]. However, *H. pylori* has modified lipid A (one step of the pathway being the removal of the Kdo sugar via Kdo hydrolase, with the final step involving the removal of the 3'-O-linked acyl chain resulting in a tetra-acylated lipid A from a hexa-acylated lipid A[17,18]) in order to minimize immune system activation, allowing for immune evasion and facilitating chronic infection[17]. The core oligosaccharide connects lipid A to the O-antigen, and the O-antigen contributes to the antigenicity of the LPS molecule[19]. The LPS of *H. pylori* helps propagate this pathogen in two ways: creating Lewis antigens to facilitate host mimicry (see details below, section 1.2.2) and immune evasion[20], and resistance to host cationic antimicrobial peptides (CAMPs) via the lipid A-core[21].
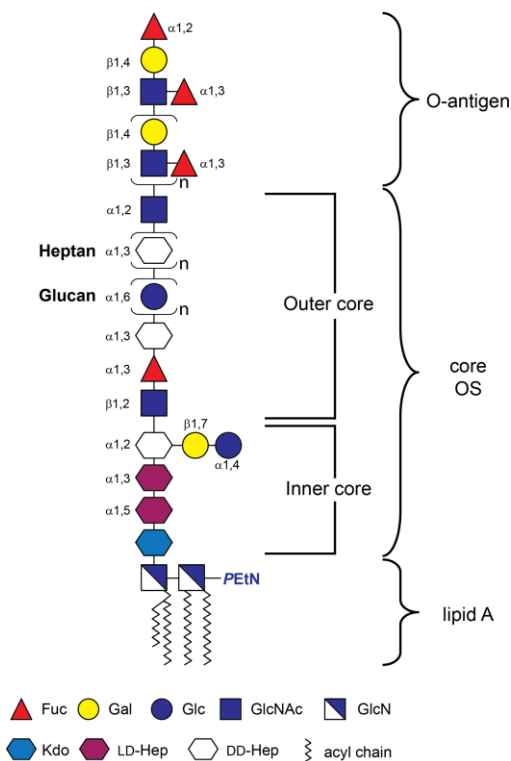
Figure 1. Proposed LPS structure of *H. pylori* reference strain 26695.
The three domains of the LPS are: the lipid A, the core oligosaccharide (divided into inner and outer core), and the O-antigen[22].

1.2.1 LPS biosynthesis

Characterizing the LPS biosynthesis pathway of *H. pylori* has not been an easy task. This is partially due to the genes involved in LPS biosynthesis being spread throughout the genome rather than organized into an operon like in most Gram-negative bacteria. However, in recent years there has been significant progress in our understanding of *H. pylori*'s LPS synthesis process.

There are three possible pathways for the biosynthesis of the O-antigen: the Wzy-dependent pathway, the ABC-transporter-dependent pathway, and the synthase dependent pathway[22], the first two being the most common. All three pathways commence in a similar fashion; WecA transfers a *N*-acetylglucosamine (GlcNAc) phosphate from UDP-

GlcNAc to undecaprenyl pyrophosphate (Und-PP)[23]. Then the three pathways differ in terms of O-antigen creation and translocation[22]. It was expected that *H. pylori* uses a Wzy-dependent pathway, in which short O-antigen units are assembled and translocated to the periplasm via Wzx flippase, where they are polymerized by Wzy into the correct length with the help of Wzz and then ligated to the lipid A-core[23]. However, no homologs for *wzx* or coding sequences for the Wzy and Wzz enzymes existed in *H. pylori*[23].

Surprisingly, *H. pylori* O-antigen synthesis follows a unique Wzk-dependent pathway (Figure 2), with Wzk being a translocase that enables the production of variable-length O-antigens[23]. In this pathway, the Und-PP-GlcNAc resulting from WecA activity acts as an acceptor for the assembly of the O-antigen. Next, glycosyltransferases add alternating Gal and GlcNAc residues to create the O-antigen backbone[23]. Then, α1,3-fucosyltransferases FutA and FutB attach fucose molecules to select GlcNAc residues, creating Lewis X. The α1,2- fucosyltransferase FutC transfers fucose to the terminal Gal to generate Lewis Y[24] (Figure 3). Notably, *H. pylori* displays a large diversity of Lewis X and Y expression on the LPS, with FutA and B acting as enzymatic rulers for fucosylation, only adding fucose to O-antigen polymers of specific lengths, based on the number of heptad repeats in the amino acid sequence of FutA and B[24]. This variability of the Lewis antigen expression pattern is likely in response to environmental changes, such as changes in pH[25] and host blood group antigens, which would promote adaptation of certain individual isolates to their host environment and facilitate further immune evasion[24]. Once assembled, the O-antigen is translocated to the periplasm by the flippase Wzk and ligated to the lipid A-core by O-antigen ligase WaaL[23]. Interestingly, the Wzk enzyme was found to be dissimilar to other translocases but homologous to *Campylobacter jejuni* (CJ) PglK, a flippase of Und-PP-heptasaccharide used for protein N-glycosylation[23,26].
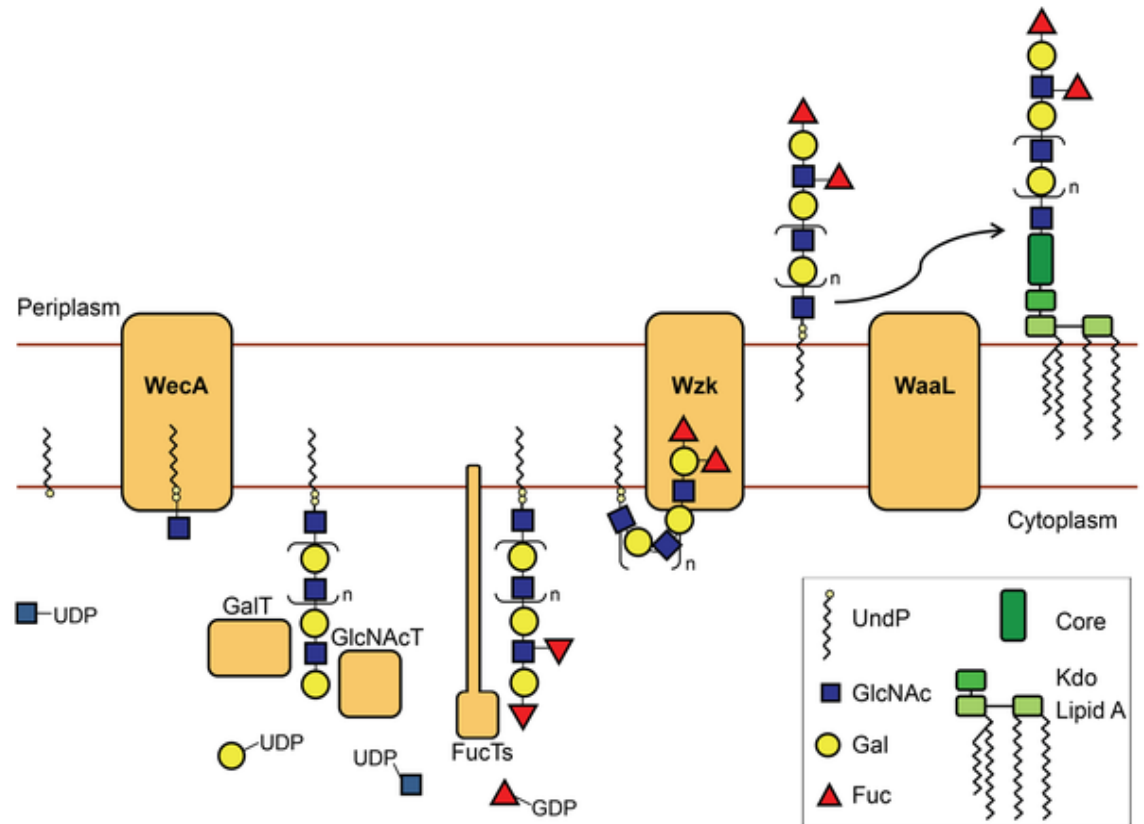
Figure 2. Novel LPS biosynthesis pathway in *H. pylori*.

LPS synthesis starts when WecA transfers GlcNAc (N-acetyl glucosamine) to UndP (undecaprenyl pyrophosphate). Next, glycosyltransferases (GalT and GlcNAcT) alternately add Gal and GlcNAc residues, producing the linear O chain backbone. Then, fucosyltransferases (FucTs) attach fucose residues on selected locations of the O-antigen backbone, generating Lewis antigens. The flippase Wzk transfers this O-antigen to the periplasm, where it is attached onto the lipid A-core via the O-antigen ligase WaaL. Once the LPS molecule is assembled, it can be transported to the outer membrane by Lpt (lipopolysaccharide transport) proteins (a transenvelope complex)[23].
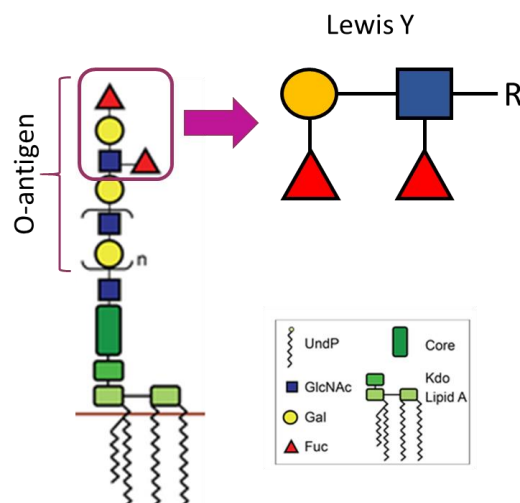
Figure 3. Enhanced view of a Lewis Y LPS structure.

The Lewis Y O-antigen is formed by the attachment of fucose to the terminal Gal in an α-1,2 linkage and to the preceding GlcNAc in an α-1,3 linkage. The R refers to the rest of the molecule. Adapted from Hug *et al*.[23] and expanded upon (Creuzenet lab)**.**

1.2.2 Lewis O-antigens and host mimicry

As introduced above, the LPS of *H. pylori* is unique in that it expresses Lewis Blood Group antigens and presents them on the O-antigen domain[20]. These are carbohydrates that are commonly associated with host monocytes, macrophages, granulocytes and gastric epithelial cells[20]. Predominantly, 80-90% of *H. pylori* strains produce type 2 blood group antigens Lewis X and Lewis Y on the LPS[27,28]. The pathogen also expresses type 1 blood group antigens Lewis A, Lewis B, Lewis C and H-antigens at a lower frequency[29]. Molecular mimicry by these antigens allows for *H. pylori*'s protection against recognition as a foreign invader and facilitates successful immune evasion[20]. However, upon recognition of the pathogen over time, this mimicry also causes an autoimmune response, leading to inflammation and tissue damage[20].

1.2.3 Phase variation

H. pylori is known to be very genetically diverse[30]. One method of increasing diversity is phase variation (or antigenic variation), in which surface epitopes, like those presented on the LPS, are reversibly switched on-and-off [31]. A proposed mechanism for phase variation is strand slippage during DNA replication in regions with homopolymeric tracts or oligonucleotide repeats[31]. The resulting products of phase variation create a microorganism that is more versatile and better able to cope in varying environmental conditions[31]. Switching on certain genes may allow this microorganism to adhere better to mucosal cells or decrease antigenicity and recognition by antibodies; switching off certain other genes may result in the reverse effect[31]. It has been determined that fucosyltransferases involved in Lewis X and Y antigen assembly undergo phase variation[31], due to their homopolymeric tract which is denoted as the frame shifting region in Figure 4.

In fact, there are a total of 27 predicted phase variable genes in *H. pylori*, several of them from the Hop outer membrane family. This includes porins HopC and HopD, HopM, and adhesin HopZ. In general, phase variation could explain the differences in isolates found within different human hosts.
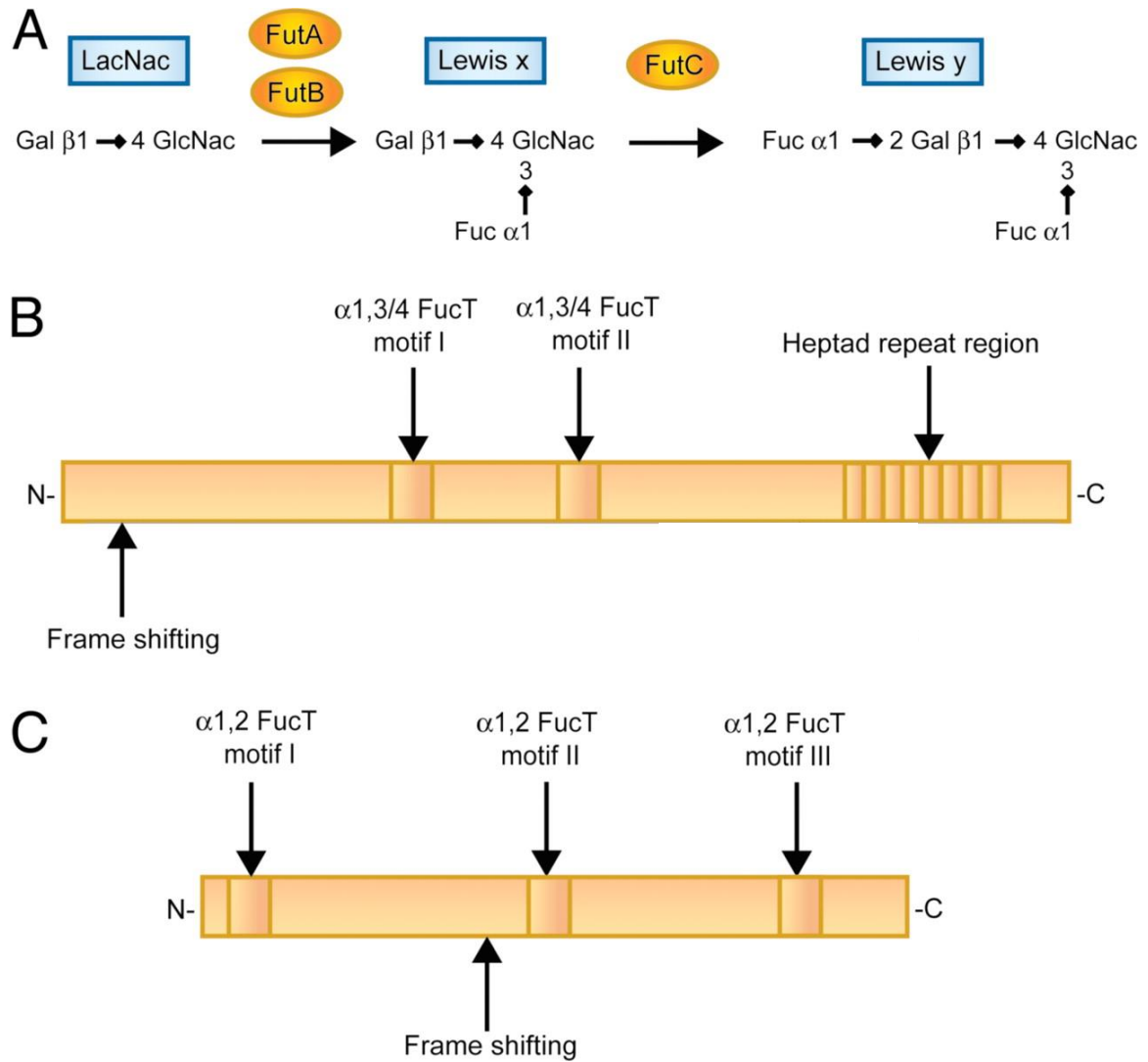
Figure 4. *H. pylori* fucosyltransferases responsible for Lewis X and Y antigens.
A) Lewis antigen structures and the pathway with enzymes involved in their synthesis. B)
FutA and B (α1,3- fucosyltransferases), indicating frame shifting in the 5' polyC tract,
with the 7 amino acid heptad region determining the size of the O-antigen polymers that
become fucosylated. C) FutC (α1,2- fucosyltransferase), frame shifting in the middle of
the gene resulting in variable expression of Lewis glycosylation[24].

1.3 *Helicobacter pylori*'s outer membrane proteins (OMPs)

Through bioinformatics analysis of *H. pylori* J99 and 26695, five paralogous gene families of outer membrane proteins (OMPs) were identified, with a total of ~64 members[32]. The largest family is comprised of 21 Hop (*H. pylori* OMP) proteins and 12 Hor (Hop related) proteins. Members of the Hop family are grouped together due to their shared or identical amino acid sequences at the N- and C- termini[32]. Family 2 contains 8 Hof (for *Helicobacter* OMP family) proteins, characterized by their similar molecular masses and hydrophobic C-terminal sequence motif present in most OMPs, and family 3 has 4 Hom (for *Helicobacter* outer membrane) proteins with conserved N- and C-termini and the C-terminal hydrophobic motif[32]. The last two families are characterized due to their homology to iron-regulated OMPs found in other bacteria, labeled FecA-like (similar to *Escherichia coli*'s ferric citrate receptor) and FecB-like (similarity to *Neisseria* spp.'s major iron-regulated OMP). Family 4 is comprised of iron-regulated OMPs (6 members) and family 5 includes efflux pump OMPs (3 members). The remaining OMPs are not members of any families (~10 members).

Five Hop members (HopA-E) from strain 26695 are characterized as porins[33], with some Hop proteins also functioning as adhesins (such as BabA and BabB)[34]. Specifically, the porin HopE (31 kDa), that is the focus of this thesis, is the smallest of these proteins and can form trimers (90 kDa)[33]. Like other porins, HopE is predicted to be a β- barrel structure, containing 16 strands with alternating hydrophobic and hydrophilic residues[35]. Forming atypically large water-filled channels for a porin, HopE has no specific binding sites and no preference for anions or cations, implying that it is a major nonspecific porin of *H. pylori* due to its lack of substrate specificity to ions[33].

1.4 *H. pylori*'s inner membrane proteins

Unlike outer membrane proteins, inner membrane proteins have not currently been characterized and quantified to the same extent in *H. pylori*. However, this section will discuss some notable inner membrane proteins.

Several of the proteins involved in LPS biosynthesis are localized within the inner membrane, such as the aforementioned WecA, the fucosyltransferases FutA and C, the O-antigen flippase Wzk, and the O-antigen ligase WaaL. Another essential inner membrane protein is UreI, part of the urease gene cluster of seven open reading frames *ureABIEFGH*, and survival of *H. pylori* in the acidic gastric environment is contingent on the expression of this inner membrane urea channel[36]. This channel conveys the gastric urea to the cytoplasmic urease, where it is hydrolyzed into carbon dioxide and ammonia, buffering the periplasm to a pH of 6.1[37].

Additionally, several putative paralogous inner membrane efflux pumps have also been identified: HefC, HefF and HefI. It is suggested that the efflux pump HefC may play a critical role in pumping out bile salts that it encounters *in vivo,* specifically in the duodenum, to prevent the antimicrobial effects of the substance[38]. Currently, the functions of HefF and HefI are unknown.

Lastly, HP0946 is a protein of interest in this thesis. Through *in silico* analysis conducted in the lab, it is a predicted inner membrane protein with 13-14 transmembrane domains (depending on the software) and is currently annotated as a sodium-proton antiporter. Additionally, our lab discovered that HP0946 shares some similarity to a well-known oligosaccharide transferase in *C. jejuni*, PglB, an enzyme that is involved in protein glycosylation. HP0946 is also predicted to have 2-3 large periplasmic loops that may interact with substrates (which can be either proteins or glycans). As such, it would be of interest to further investigate the function of HP0946 and determine if there is any connection to the LPS biosynthesis pathway, potentially by interacting with the Lewis substrate and leading to glycosylation of protein(s) with this substrate.

1.5 Protein glycosylation

Protein glycosylation is characterized as the modification of proteins through covalent attachment of carbohydrates[39]. Initially, it was thought that protein glycosylation existed only in eukaryotes, however it is now well established that protein glycosylation occurs in prokaryotes and archaea as well. These modifications are critical for a wide range of biological processes, such as controlling protein folding and protein stability[40], regulating intracellular trafficking, modulating enzyme and hormone activities, participation in cell-cell interactions, and acting as cell surface receptors[41].

There are two main types of protein glycosylation: N-linked and O-linked. N-glycosylation occurs via linkage of a glycan (such as GlcNAc or other) to the nitrogen in the amido group of asparagine, whereas O-glycosylation occurs when a glycan (i.e. *N*-acetylgalactosamine, GalNAc or other) is attached to the oxygen in the hydroxyl group in either serine or threonine[42].

The sites at which glycosylation takes place depends on the specific sequence of amino acids adjacent to either asparagine (Asn), serine (Ser) or threonine (Thr)[42]. The consensus sequence for N-glycosylation is either Asn-X-Thr/Ser (with X being any amino acid except proline)[42]. This is a well conserved sequence in eukaryotes, however prokaryotes likely have an extension of this glycosylation sequence. Bacteria such as *Campylobacter jejuni* require an extended glycosylation sequence, which is as follows: Asp/Glu-Y-Asn-X-Ser/Thr (where X and Y are not proline)[43]. No widespread consensus sequence has been determined for O-glycosylation[42], however one lab was able to determine the conserved sequence in intestinal *Bacteroides* species, *Bacteroides fragilis*, as being Asp-Ser/Thr-Ala/Ile/Val/Met/Thr (the last amino acid must contain either one or more methyl groups)[44]. To date, only *Campylobacter jejuni* has been found to carry both N- and O-protein glycosylation pathways[45].

1.5.1   Protein glycosylation in eukaryotes

First discovered in eukaryotes, it is now predicted that more than two-thirds of eukaryotic proteins undergo protein glycosylation[46]. Regardless of the eukaryote, the biosynthetic machinery responsible for this modification follows a similar progression.

The eukaryotic N-glycosylation pathway starts with the assembly of the glycan in the cytoplasm of the endoplasmic reticulum (ER) and is mediated by the membrane-embedded dolichol pyrophosphate lipid carrier. The glycan is extended through the addition of sugar molecules by embedded glycosyltransferases in a step-wise manner to form the precursor oligosaccharide. Next, the glycan is translocated across the membrane to the ER lumen by a currently unknown flippase protein, where the oligosaccharide decoration is resumed by more glycosyltransferases on the lumen side and results in the production of a conserved tetradecasaccharide ($Glc_3Man_9GlcNAc_2$) core oligosaccharide. This final oligosaccharide is then transferred *en bloc* to the target protein by an N-oligosaccharide transferase (N-OST)[47].

Comparatively, the process of eukaryotic O-glycosylation is much more variable; currently, no dedicated O-glycosylation pathway has been identified. Although most O-glycosylation occurs in the Golgi apparatus, some O-glycosylation has been found to be initiated in the ER. O-glycosylation begins with the addition of monosaccharide (commonly N-acetyl-galactosamine, GalNAc) to the protein by a glycosyltransferase, followed by sequential addition of more sugars (such as fucose, mannose, and glucose) to form the final glycan[48]. Regardless of the discrepancies, both forms of eukaryotic glycosylation contribute to the wide range of protein diversity.

1.5.2 Protein glycosylation in prokaryotes

Since the discovery of surface layer (S-layer) glycoproteins in a Gram-negative halophile, *Halobacterium salinarium* in the 1970s[49], it has been well established that prokaryotes also go through this modification, such as *C. jejuni*[50] and *H. pylori*[51]. In fact, the first N-linked protein glycosylation was discovered in *C. jejuni*[52].

More than 60 N-glycoproteins have been identified in *C. jejuni*[53]. As the model system for bacterial N-glycosylation, glycosylation initiates when a heptasaccharide is assembled (one sugar at a time) to an undecaprenyl pyrophosphate on the cytoplasmic side of the inner membrane. The assembled lipid-linked oligosaccharide is then flipped across the inner membrane to the periplasm by an ATP-dependent flippase, PglK[54], similar to eukaryotic N-glycosylation. Then, an oligosaccharide transferase (OST), PglB[55], transfers the glycan to an asparagine residue on the acceptor protein. Mutations within this pathway in *C. jejuni* have been shown to reduce chicken colonization[56], adherence ability, and diminish the ability to invade intestinal epithelial cells *in vitro*[57].

Similar to N-glycosylation, O-glycosylation has been described in several bacteria and archaea. O-glycosylation is well known to occur on bacterial surface appendages, such as flagella and pili. Focusing on *C. jejuni* again, O-linked glycan modification of the flagella is necessary for flagellum assembly, and can affect auto-agglutination, biofilm formation and colonization of the gastrointestinal tract[58]. The O-linked glycans on the flagellar proteins can constitute up to 10% of the protein mass[50]. Predominantly, the O-glycans attached to the flagellum are pseudaminic acid (PA) or legionomic acid derivatives[59,60].

Unlike the *en bloc* transfer of glycans in N-glycosylation pathways, flagellin O-glycosylation mainly occurs in a sequential pattern. In this case, glycosyltransferases sequentially transfer monosaccharides to the target protein. Once completed, the glycosylated flagellin monomers are secreted to the tip of the growing flagellin unit. This form of O-glycosylation is OST-independent and is generally used to glycosylate flagellins and non-pilus adhesins such as autotransporters[61].

Similar to the N-glycosylation pathway described in *C. jejuni*, OST-dependent O-glycosylation is used to glycosylate the type IV pilus of *Neisseria gonorrhoeae* and *Neisseria meningitidis*. This pathway is initiated when the glycosyltransferase attaches a monosaccharide to the undecaprenolphosphate (Und-P) lipid carrier located on the inner side of the plasma membrane. Then, glycosyltransferases attach more monosaccharides to this precursor. Once completed, the Und-P linked glycan is flipped to the periplasm and an OST transfers this glycan to the target protein[62]. In addition to being similar to the N-glycosylation pathway, this general O-glycosylation also has similarities to the Wzy-dependent pathway involved in the production of LPS O-antigen synthesis[23]. Overall, O-glycosylation is widespread and not the rare event it was previously perceived to be. However, there are still many enzymes in this pathway that have not been identified and characterized.

1.5.2.1   Outer membrane protein glycosylation in prokaryotes

Currently, two bacterial porins have been identified as glycoproteins. Previous research regarding a porin in *Campylobacter jejuni*, major outer membrane protein (MOMP), showed that the MOMP is O-glycosylated with a glycan moiety containing one galactose and three GalNAc residues at T268, which is in a surface exposed loop, with this glycosylation resulting in a conformational change of MOMP[63]. The glycosylation of this porin either directly or indirectly promoted cell-to-cell binding, biofilm formation, adhesion to Caco-2 cells, and was necessary for *C. jejuni*'s optimal colonization of chickens[63].

The second porin, OprD of *Pseudomonas aeruginosa*, is a β-barrel shaped channel-forming porin which uptakes basic amino acids, peptides and β-lactam antibiotics. It is highly sialylated, resulting in lower penetration of β-lactam antibiotics through this porin, indicating this may be a novel mechanism of drug resistance[64]. Thus, it is possible that glycosylation of HopE may also contribute to antibiotic resistance.

1.6 *Helicobacter pylori* and protein glycosylation

To date, characterizing novel protein glycosylation pathways in *H. pylori* and its role on protein function has been elusive. Currently, it is known that flagellins FlaA and FlaB that comprise of the flagellar filaments are O-glycosylated with pseudaminic acid, which is essential for the production of the flagellum and virulence of the pathogen[51].

Interestingly, mounting evidence from three individual labs suggests a connection between flagellin glycosylation and LPS O-antigen biosynthesis in *Aeromonas caviae*[65], *Helicobacter pylori*[66], and *Pseudomonas aeruginosa*[67]. Specifically, in *H. pylori*, the FlaA1 enzyme is involved in the pseudaminic acid synthesis pathway for the glycosylation of flagella[51,68]. This enzyme was implicated in functionally linking the control of LPS biosynthesis and flagellum production, with protein glycosylation being the underlying mechanism for this interconnection[66]. Further evidence for a link in the two machineries is identified by the aforementioned flippase Wzk, that is homologous to *Campylobacter jejuni'*s PglK enzyme that is involved in N-glycosylation[26]. The last piece of evidence stems from our unpublished lab data, in which a connection was discovered between two proteins of interest in this thesis: the O-antigen ligase WaaL, HP0946 (a putative Lewis Y oligosaccharide transferase) and FlaA1 via RT-qPCR. HP0946 transcription expression levels were upregulated in mutants that tend to increase Lewis Y availability: 7-fold in a *waaL* mutant that is unable to attach O-units for LPS assembly and 10-fold in a *flaA1* mutant that cannot utilize Und-PP-GlcNAc, a component of Lewis antigen synthesis[66].

Previously, the Creuzenet lab determined that the pseudaminic acid pathway is not limited to *H. pylori*'s flagellin production, but also targets proteins involved with virulence factor production, such as LPS and urease[45]. The data also identified several non-flagellar glycoproteins using glyco-specific stains, digoxigenin-3-O-succinly-ε-aminocaproic acid hydrazide (DIG) labelling and mass spectrometry (MS)[45]. This idea that non-flagellar proteins are glycosylated in *H. pylori* had also been proposed concurrently by another lab based on global metabolic profiling, but in that study the glycoprotein (GP) candidates had not been isolated or characterized[69]. In the Creuzenet lab, identification was conducted on 9 GP candidates, which were the most abundant.

One of the GP candidates was determined to be catalase, whose glycosylation had never been reported before. The other GP candidates were presumed to be linked to LPS biosynthetic enzymes, since PA mutants expressed altered or no O-antigens[45]. Through further research with wild-type and PA mutants, it was concluded that there may be several glycosylation pathways in *H. pylori*[45].

Evidence of glycosylation of non-flagellar proteins in *H. pylori* was further corroborated by another lab. Using a combination of metabolic glycan labelling (supplementing the strain with peracylated *N*-azidoacetylglucosamine, Ac$_4$GlcNaz, leading to labelling of the N-linked and O-linked glycoproteins with azide), MS analysis, and Western blotting, this lab was able to identify the existence of 125 putative GPs in *H. pylori*[70]. These results revealed that GPs are abundant and widespread in *H. pylori*, existing on the cell surface, inner and outer membranes, and within the periplasm and cytoplasm[70]. This distribution suggests that protein glycosylation may be an essential process of *H. pylori*'s physiology, with intracellular glycans potentially being involved in stabilizing proteins and extracellular glycans stabilizing proteins and mediating host-cell interactions[70].

While these 125 proteins comprise those previously identified in the Creuzenet lab, they do not comprise the outer membrane protein HopE that is the focus of this study. One reason for this would be the nature of HopE glycosylation. Based on the sugar chemistry of metabolic labelling, the GlcNac to be labelled would have to be on the base of the polysaccharide structure. Although GlcNac in *H. pylori* is the initiating (base) sugar in the process of LPS synthesis (and HopE glycosylation may happen by attachment of this LPS O-antigen to the HopE protein), OSTs are usually specific for the motif they recognize and transfer to the protein. Thus, the Lewis Y OST may not transfer this single initiating base GlcNac, and there would be no guarantee that metabolic labelling would aid in the identification of HopE.

Recently, using biotin-hydrazide labeling, anti-Lewis Western blotting, and silver staining of outer membranes, our lab discovered that *H. pylori* strain NCTC 11637 contained a ~31 kDa Lewis Y glycoprotein. MS and enrichment by lectin affinity

chromatography potentially identified this protein as the HopE porin that may be glycosylated by a Lewis Y antigen. To confirm this, a *hopE* knockout mutant was constructed, and anti-Lewis Y Western blotting of the outer membranes determined that this ~31 kDa protein was present in the wild-type but absent in the knockout mutant. The MS data also identified a putative glycopeptide that partially matched the amino acid sequence of HopE, and which had 3 potential glycosylation sites: O-glycosylation on a serine or threonine, and a N-glycosylation consensus sequence reading as Asn-Ala-Thr. Modelling by Dr. Creuzenet (using the program Swiss-Prot against *P. aeruginosa*'s OprH) indicated that this putative glycopeptide was localized on the surface of the outer membrane, implicating its possible role in host mimicry, immune evasion, or adhesion to host tissues (Figure 5).
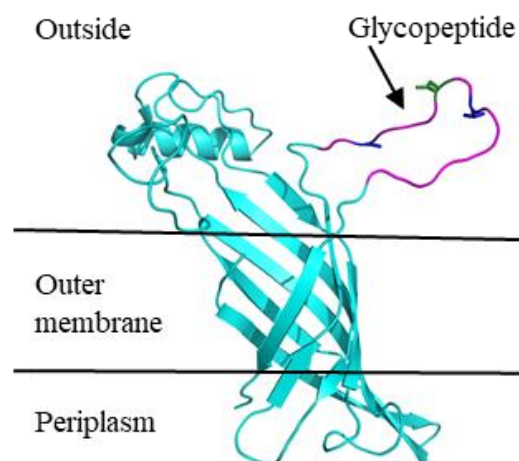
Figure 5. Three-dimensional model of HopE.
HopE is likely glycosylated on the purple surface exposed loop as per preliminary mass spectrometry data. Approximate boundaries of the hydrophobic regions of the proteins predicted to be embedded in the outer membrane are represented by horizontal lines. Modelled by Dr. Creuzenet.

1.7 Hypothesis and objectives

Based on the above evidence, we propose that: The HopE porin in *H. pylori* plays a role in antibiotic susceptibility, which may be influenced by HopE glycosylation with a Lewis O-antigen transferred by the putative oligosaccharide transferase HP0946. Collectively, this contributes to the pathogen's virulence.

To address this hypothesis, we have three objectives:

1) Optimize the detection of HopE using anti-HopE antibodies to determine whether HopE is glycosylated, via anti-Lewis Western blotting.

2) Investigate the role of the Lewis oligosaccharide transferase HP0946 in potential HopE glycosylation and determine its connection to LPS synthesis.

3) Elucidate the functional impact of HopE and its putative Lewis glycosylation in regard to antibiotic resistance/susceptibility.

Chapter 2: Materials and Methods

2 Materials and methods

2.1 Bacterial strains and growth conditions

All *Helicobacter pylori* NCTC 11637 strains were grown under microaerobic conditions (5% O_2, 10% CO_2, and 85% N_2) and 90% humidity in a tri-gas incubator (NuAire) for 48 hours on Columbia agar (Fisher Scientific) plates supplemented with 7.5% sheep blood (Cedarlane), 0.05 µg/mL sodium pyruvate (BioShop), 5 µg/mL trimethoprim (Sigma-Aldrich), 10 µg/mL vancomycin (Bio Basic), and 4 µg/mL amphotericin B (Bio Basic); these are considered the "background" antibiotics. When growing knockout strains, the agar was supplemented for selection with 5 µg/mL of kanamycin (Bio Basic) and/or 12 µg/mL of chloramphenicol (Fisher Scientific). *H. pylori* cells were stored as freezer stocks kept at -80°C in brain heart infusion yeast extract (BHI-YE) media (EMD and Fisher Scientific) with 25% glycerol (Fisher Scientific) and the appropriate antibiotics/supplement. After initial revival from a loopful of freezer stock onto Columbia agar plates, the cells were spread onto a new plate via sterile loop and grown for 48 hours. The confluent lawn was resuspended in BHI-YE broth with no supplement or antibiotics and normalized to an OD_{600} of 0.2 before being spread to new Columbia agar plates with no selection antibiotics via sterile cotton swabs. After 48 hours, the cells were harvested to an OD_{600} of 0.5 before downstream phenotypic analyses. Table 1 shows the list of strains used in this study.

Table 1. *Helicobacter pylori* **strains used.**

Strain	Gene(s) disrupted	Antibiotic cassette	Made by
VJ WT	None	---	Used by V. Somalinga
VJ Δ*hopE*	*hopE*	Chloramphenicol	K. Yogendirarajah (in this study)
MK WT	None	---	Used by M. Khodai-Kalaki
BO Δ*hopE*	*hopE*	Chloramphenicol	B. Oickle
Δ*946*	*946*	Kanamycin	J. Denomme
Δ*hopE*/Δ*946*	*hopE* and *946*	Chloramphenicol and kanamycin	K. Yogendirarajah (in this study)
Δ*waaL*	*waaL*	Kanamycin	A. Merkx-Jacques
Δ*hopE*/Δ*waaL*	*hopE* and *waaL*	Chloramphenicol and kanamycin	K. Yogendirarajah (in this study)

Escherichia coli DH5α cells were grown in Luria Bertani (LB) broth (BioShop) in a 37°C shaking incubator at 133 rpm (New Brunswick Scientific) in standard atmospheric conditions. The broth was supplemented with 100 µg/mL ampicillin (Bio Basic) and/or selection antibiotics of either 34 µg/mL chloramphenicol or 30 µg/mL kanamycin.

2.2   Membrane fractionation by differential solubilization

H. pylori cells were revived and subsequently grown and expanded to 20 plates of confluent growth. Cells were re-suspended in 5 ml of 0.85% saline and lysed in a cell disrupter (Constant Systems LTD IS6/40/BA/AA model) at 25,000 psi. Cellular debris and unlysed cells were pelleted by centrifugation at 5,000 *g* for 20 min. The supernatant was removed and ultracentrifuged for 1 hour at 100,000 *g* at 4°C to pellet membrane

proteins (Optima-XL 100K ultracentrifuge, Beckman Coulter, TLA 110 rotor). The recovered total membrane pellet was resuspended in 1 mL of 0.85% saline and ultracentrifuged again for 1 hour under the same conditions as previously mentioned. Then, the total membrane pellet was resuspended in 1 mL of solubilization buffer (50 mM sodium phosphate, 300 mM NaCl, pH 7.2) containing 1% w/v N-laurylsarcosine (Sigma-Aldrich) and mixed on a nutator for 1 hour at room temperature and overnight at 4°C. The outer membrane was pelleted from the inner membrane via ultracentrifugation at 100,000 g for 1 h at 4ºC. The outer membrane pellet was mixed again with solubilization buffer to further remove any leftover non-outer membrane components. The final clean outer membrane pellet was resuspended in PBS (50 mM sodium phosphate, 300 mM NaCl, pH 7.2) for protein analysis via SDS-PAGE.

2.3   Proteinase K digestion

For experiments that required complete protein degradation, outer membrane and total membrane protein samples were digested with Proteinase K (PK). To 120 µL of total protein samples, 5 µL of 20 mg/mL PK (BioShop) was added, while 30 µL of outer membrane samples were supplemented with 2 µL of 20 mg/mL PK. Samples were incubated at 60°C overnight to ensure completed digestion.

2.4 Western blotting and SDS-PAGE analysis

Bacterial cells were denatured with 1X SDS loading buffer (0.625 M Tris, 2% SDS, 2% β-mercaptoethanol, 10% glycerol, 0.002% bromophenol blue, pH 6.8) and incubated for 5 min at 100°C. The proteins were separated by SDS polyacrylamide gels in the Laemmli system (Bio-Rad mini gel system). The gels used varied depending on the application and included 12% bis-acrylamide gels (made in lab), bis-acrylamide step-wise gels (12% in the bottom third of the gel, 15% in the middle and 20% at the top; made in lab), and pre-cast gradient gels (4-20% bis-acrylamide, Bio-Rad). Lab-made gels were electrophoresed at 30 mA, while pre-cast gels were run at 250 V in 1X tris-glycine

buffer (0.025 M Tris, 0.192 M glycine, 0.1% SDS, pH 8.3). Proteins and carbohydrates were visualized either via silver staining or Western blotting. Proteins were occasionally also visualized by Coomassie blue staining (10% acetic acid, 25% ethanol, 0.001% w/v Brilliant Blue R-250 (Bio-Rad). Antibodies, lectin and Western blotting conditions used are explained in Table 2.

For Western blotting, proteins were transferred to nitrocellulose membrane (Bio-Rad) via wet transfer for 45 min at 180 mA in cold tris-glycine transfer buffer (25 mM Tris, 192 mM glycine, 10% methanol, pH 8.3). After transfer, the proteins on the membrane were visualized with Ponceau S stain (0.1% w/v Ponceau S (Sigma-Aldrich) and 1% v/v acetic acid) for 2 min and washed with milliQ water. The membrane was blocked for 1 hour with 10% skim milk with gentle shaking on the gel surfer (Diamed). All further steps were performed with this gentle shaking. The membrane was then washed twice with phosphate buffered saline (PBS) buffer (137 mM NaCl, 2.7 mM KCl, 8 mM Na_2HPO_4, 1.46 mM KH_2PO_4, pH 7.2) supplemented with 0.05% Tween-20 (USB Corporation), and once in PBS buffer for 10 min each. Then, the membranes were incubated with primary antibody for 1 hour. After incubation, the membrane was washed as previously mentioned, then incubated with secondary antibody for 35 min in the dark. The membrane was washed in the dark as stated above. Protein or LPS was visualized using the Odyssey CLx imaging system (Li-Cor) at the wavelengths mentioned in Table 2.

Western blots were performed to screen aliquots of rabbit anti-HopE antibody sera from different bleeds at different concentrations to determine optimal conditions for future Western blotting. The outer membranes WT and Δ*hopE* samples were separated by step-wise gels (with a single large well) and transferred to nitrocellulose membranes as stated above. After transfer and Ponceau S staining of total protein content, the membranes were cut length-wise into 7 identical strips and each strip was individually blotted with the different bleeds (bleed #2, #3, #4) and the pre-immune serum. The strips were then washed, blotted with the secondary antibody, and imaged as previously mentioned.

Table 2. Western blotting reagents used.

Epitope detected	Primary antibody/lectin	Secondary antibody	Wavelength detection (nm)
HopE	Anti-HopE (1/200) rabbit (ProSci) [Custom ordered]	Goat anti-rabbit IRDye (1/5000) (Li-Cor)	800
Lewis Y	Anti-Lewis Y (1/100) mouse (Calbiochem)	Anti-mouse (1/5000) goat AlexaFluoro 680 (Invitrogen)	700
Fucose	BambL lectin (biotinylated by the Creuzenet lab)	Streptavidin conjugated AlexaFluoro 680 (Invitrogen) 1µg/mL	700

2.5   Silver staining of carbohydrates

The following silver staining protocol was created by Fomsgaard et al[71]. Briefly, carbohydrates were first separated on an SDS-PAGE and then oxidized in a solution of 0.7% w/v periodic acid, 40% v/v ethanol and 5% v/v acetic acid in milliQ water with shaking for 20 min. The oxidation was followed by five washes over 15 min in milliQ water. The gel was then stained with silver nitrate (Fisher Scientific) in a staining solution (0.19% v/v 10 N NaOH, 1.3% v/v ammonium hydroxide, 0.7% w/v silver nitrate). Gels were stained for 10 min, followed by five washes over 15 min in milliQ water. Following the wash, the gels were developed using 0.005% w/v citric acid and 0.05% v/v formaldehyde (37%) in milliQ water until bands became visible. The gels were then washed several times with milliQ water and scanned.

2.6   Chromosomal DNA extraction from *H. pylori*

Chromosomal DNA was extracted from total cell pellets using the cetyltrimethylammonium bromide (CTAB) buffer (100 mM Tris-HCl, 1.4 M NaCl, 0.02 M EDTA, 1% w/v CTAB (BioBasic), pH 8.8) method. To the cell pellet, 500 µL of 1% CTAB buffer and 500 µL of phenol:chloroform:isoamyl alcohol (25:24:1 v/v/v) was added and vortexed to mix the solutions until an emulsion formed. This mixture was centrifuged at 13,000 *g* for 5 min. The top aqueous layer was extracted and 500 µL of chloroform-isoamyl alcohol (24:1) was added and centrifuged at 13,000 *g* for 5 min to remove residual phenol. The top aqueous phase was recovered, and the DNA was precipitated by adding 0.08 volume of chilled 3 M potassium acetate and 0.54 volume of chilled isopropanol. The tubes with the mixture were inverted 30 times and incubated on ice for 35 min. The DNA was pelleted by centrifugation at 13,000 *g* for 10 min at 4°C. The DNA pellet was washed once with cold 100% ethanol, centrifuged as before, and washed once again with cold 70% ethanol and air dried. The final DNA pellet was resuspended in 50 µL of autoclaved TE buffer (50 mM Tris-HCl, 2 mM EDTA, pH 8) and stored at 4°C.

2.7   Agarose gel electrophoresis

All PCR products were analyzed using 0.7% agarose gel prepared in TAE buffer (40 mM Tris-acetate, 1 mM EDTA, pH 8.0). Samples were mixed with DNA loading buffer (1X TAE buffer, 12.5% glycerol, 0.0025% bromophenol blue) before loading and compared to a 1 kb DNA ladder standard (Invitrogen). Ten µL of ethidium bromide (Invitrogen) were added to the gel tank before running the gel. Gel electrophoresis was performed at 80 V for 30 min. DNA bands were visualized using UV light (254 nm) in the Quantity One Chemidoc XRS system.

2.8 Transformation of pUC18/706KO into *H. pylori* NCTC11637 strains

The appropriate *H. pylori* strain was grown under microaerobic conditions as described above and the cells were harvested into BHI-YE broth, pelleted at 4,000 rpm for 10 minutes and washed twice in 0.85% saline, with centrifugation steps in between. The cells were then adjusted to an OD_{600} of 0.5 in 0.85% saline. A total of 20 µg of plasmid DNA was added to the cells to a final volume of 100 µL. A negative transformation control consisted of 100 µL of cells with no plasmid incorporated. The transformation mixtures were spotted onto Columbia agar plates supplemented with 7.5% sheep blood, containing the antibiotics necessary for the original strain (WT or mutant knockout) and cells were allowed to recover for 8 hours under microaerobic conditions at 37°C. The spots were resuspended in BHI-YE broth and plated onto Columbia agar plates containing the appropriate antibiotics for selection using glass beads. Plating onto Columbia agar plates with no antibiotics, to ensure viability after transformation, was also done in parallel. These plates were grown for 5-7 days under microaerobic conditions at 37°C until colonies were observed.

2.9 Minimum Inhibitory Concentration (MIC) E-strips

As mentioned in section 2.1, once the strains have been diluted to an OD_{600} of 0.5 in 0.85% saline, the suspension was spread with a sterile cotton swab onto Columbia agar plates (with 7.5% sheep's blood and no background/selection antibiotics or pyruvate). Without re-dipping in the suspension, the plates were swabbed twice more after rotating the plate 120° each time. After letting the plates dry for 2 min at atmosphere conditions, the antibiotic E-test strip (Oxoid) was removed from its packet with clean forceps and gently placed into the centre of each plate, being careful not to introduce bubbles between the strip and the agar. Plates were incubated in microaerobic conditions in the 37°C incubator for 48 hours. After incubation, the MIC was read off the strip.

2.10   Disk diffusion assay

The antibiotic disks used in this assay were made in lab. Using a hole puncher to create the disk shape, Bio-Dot SF filter paper (Bio-Rad) was cut and sterilized under UV light. Once the appropriate concentrations of the clarithromycin antibiotic were calculated, 10 uL of the solution was added onto the disks, dried, and stored at 4°C.

H. pylori strains were adjusted to an OD$_{600}$ of 0.5 in 0.85% saline. The plates were swabbed as per section 2.8 above and then left to dry for 2 min at atmosphere conditions. Once dried, the plate was divided in half (one half per antibiotic concentration to be tested) and the disks were placed with clean forceps in the center of the appropriate section of the plate. After incubating the plate for 48 hours in microaerobic conditions at 37°C, the diameter of the zone of inhibition was measured using a ruler (in millimetres).

2.11   Immunoprecipitation of HopE

HopE polyclonal IgG antibodies immobilized to protein G agarose beads (Roche Diagnostics) were used to pulldown and purify the HopE protein from the outer membrane protein sample.

To prepare for binding, 400 µL of the beads were washed with 0.1 M sodium phosphate buffer (PB) at pH 7.4, and were incubated with 100 µL anti-HopE rabbit serum and 320 µL of 0.1 M PB at 4°C with agitation for 30 min. The beads were then washed three times with 0.1 M PB. The protein G immobilized antibodies were washed with 0.2 M triethanolamine (Sigma-Aldrich) buffer, which allows for the optimal crosslinking activity of dimethyl pimelimidate (DMP). Cross-linking buffer containing 0.2 M triethanolamine and 22 mM of DMP (Sigma-Aldrich) was then added and allowed to incubate for 45 min at room temperature. Next, 0.1 M ethanolamine (Fisher Scientific) blocking buffer (pH 7.4) was added to quench the cross-linking reaction, and the solution was left for 1 hour at room temperature with agitation to incubate. Finally, 1 mL of 0.1 M glycine-HCl (pH 2.5) elution buffer was used to remove any non-cross-linked IgG molecules from the protein G beads and immediately washed with 0.1 M PB after the

beads settled to the bottom of the tube. The beads were washed twice with PB to clear the beads of elution buffer and detached IgG molecules.

To further solubilize the partially insoluble VJ WT outer membrane sample in this experiment, 240 µL of 0.1 M PB with 0.2% Triton X-100 (Mallinckrodt) was added to 160 µL of VJ WT outer membrane sample. The sample volume used for this experiment was determined from previous Western blots that used the original OD_{600} of the VJ WT outer membrane stock (which was 47.7 from 20 plates). The sample mix was incubated at room temperature with gentle shaking for 30 min. The solution was ultracentrifuged at 100,000 g for 1 hour at 4°C and the supernatant was removed and diluted by half with 0.1M PB to a concentration of 0.1% Triton X-100. The leftover pellet was resuspended in 0.1M PB with 1.0% Triton X-100 and ultracentrifuged as before, and the supernatant was diluted to a concentration of 0.1% Triton X-100. The pellet was kept and labelled "OM unlysed".

The lysed outer membrane mixture and the prepared anti-HopE protein G beads were incubated overnight at 4°C with gentle agitation. To perform the pulldown, the resulting protein and bead mix were transferred to a Nanosep 3K omega centricon tube (Pall Corporation). This tube was used as separating the beads from the surrounding solution proved difficult in the previous steps of this experiment, resulting in a minor loss of beads each time supernatant was removed. It was expected that using a centricon tube would prevent loss of beads as the solution could pass through the membrane unimpeded and separate from the beads.

After the overnight incubation, the beads were then centrifuged as according to centricon manufacturer instruction, at 13,000 g at 4°C for 15 minutes for the supernatant to be removed. The supernatant was labelled "Unbound". The beads were washed three more times in 0.1 M PB containing 0.1% Triton X (to prevent aggregation and maintain protein solubilization). Before the elution step, the beads were changed to a Nanosep 30K omega centricon tube to allow the HopE protein to pass through the membrane and into the filtrate receiver. To elute the HopE protein from the antibody complex, 100 µL of 0.1 M glycine HCl (pH 2.5) was added to the beads and the tube was centrifuged at 5,000 g

for 5 min at 4ºC. The supernatant was recovered ("Elution") and the acidity quenched with an equivalent amount of 1N NaOH and checked with pH strips to ensure a neutral pH. The elutions were analyzed on a Western blot.

2.12 Statistical analysis

Raw data was input into Graphpad Prism 6 software and all calculations including means and standard errors and statistical analyses were performed using this software.

Chapter 3: Results

3   Results

3.1   Optimization of the detection of HopE using anti-HopE antibodies

Rationale:

Previously, using biotin-hydrazide labeling, anti-Lewis Western blotting, and silver staining of outer membranes, our lab discovered that *H. pylori* (HP) strain NCTC 11637 contained a ~31 kDa Lewis Y glycoprotein. Mass spectrometry and enrichment by lectin affinity chromatography potentially identified this protein as the HopE porin that may be glycosylated by a Lewis Y antigen. To confirm this, a *hopE* knockout mutant was constructed; anti-Lewis Y Western blotting of the outer membranes determined that this ~31 kDa protein was present in the wild-type but absent in the knockout mutant. The MS data also identified a putative glycopeptide that partially matched the amino acid sequence of HopE which had 3 potential glycosylation sites: O-glycosylation on a serine or threonine, and a N-glycosylation consensus sequence reading as Asn-Ala-Thr. Modelling by Dr. Creuzenet (Figure 5) indicated that this putative glycopeptide was likely localized on the surface of the outer membrane, implicating its possible role in host mimicry, immune evasion, or adhesion to host tissues.

However, at that time there were no antibodies to detect the HopE and verify if it was HopE that was reacting to the anti-Lewis Y antibodies. To overcome this problem, Dr. Creuzenet ordered rabbit antibodies (from ProSci Inc.) against a portion of HopE, specifically a 15-amino acid sequence relating to a surface-exposed peptide loop: GYKKFFQFKSLDMTS. This section of HopE was chosen for a several reasons. Firstly, we needed the epitope to be from a portion of HopE that faced the outside of the cell, in order to use this antibody for detecting the protein when subjected to whole cells. This would be useful, for example, if the antibody is to be used to probe for interactions between the HP and gastric cells. Secondly, the epitope also needed to be on an area that was not near the location of the glycan, to prevent masking of that location if the Western blot was re-probed with anti-Lewis Y. Lastly, this epitope was one of the few acceptable locations that was found to be immunogenic according to *in silico* analysis.

Results:

Two rabbits were immunized against this amino acid sequence (rabbit #1 and #2). The ELISA titer results, obtained from the serum supplier, for the final bleed showed that rabbit #1 had a lower ELISA titer than rabbit #2. Thus, we began working to optimize the antibody detection of HopE on Western blot using the serum from rabbit #2 (Figure 6).

Dilutions	(Rabbit 1) Pre-bleed	Final bleed	(Rabbit 2) Pre-bleed	Final Bleed
1:1,000	0.061	2.448	0.052	2.633
1:5,000	0.049	1.301	0.049	1.622
1:25,000	0.048	0.466	0.049	0.774
1:125,000	N/A	0.141	N/A	0.222
1:625,000	N/A	0.074	N/A	0.122
ELISA TITER	N/A	>1:123,400	N/A	>1:492,200
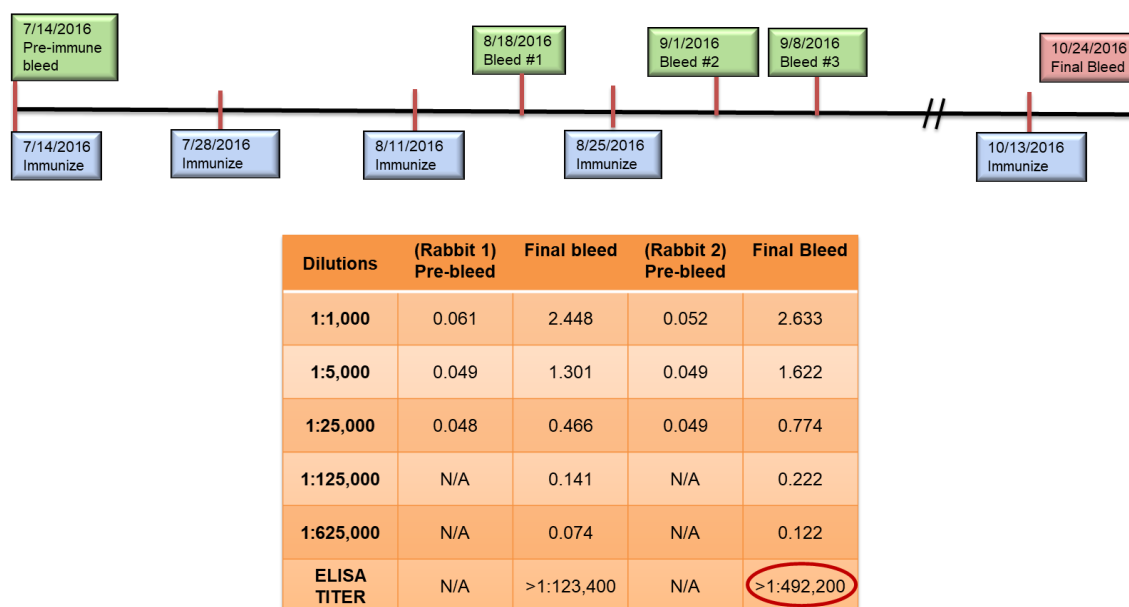
Figure 6. Timeline of polyclonal antibody production and ELISA results for both rabbits.

Two pathogen-specific free rabbits were immunized with the HopE epitope multiple times over a period of months. The ELISA titer results were quantified by ProSci and compared the pre-bleed versus the final bleed for both rabbit sera. The red circle in the ELISA table points out the larger antibody titer in rabbit #2.

As we did not know which bleed would give us the best detection of the HopE protein without much background signal, and at which dilution, we tested all bleeds at various dilutions, ranging from 1/200 to 1/1000. The pre-immune serum was used as a comparison against the three bleeds; it was not exposed to the HopE peptide so the antibodies from the pre-immune serum should not react to HopE. We also only used outer membrane (OM) samples (separated from the rest of the bacterial components using ultracentrifugation and differential solubilization with N-laurylsarcosine), as we knew HopE was an outer membrane porin, in order to minimize background signals and enrich the protein of interest. To better resolve proteins of lower molecular weight (MW), we created a stepwise gel and ran the OM samples of WT and the *hopE* knockout mutant (Figure 7).
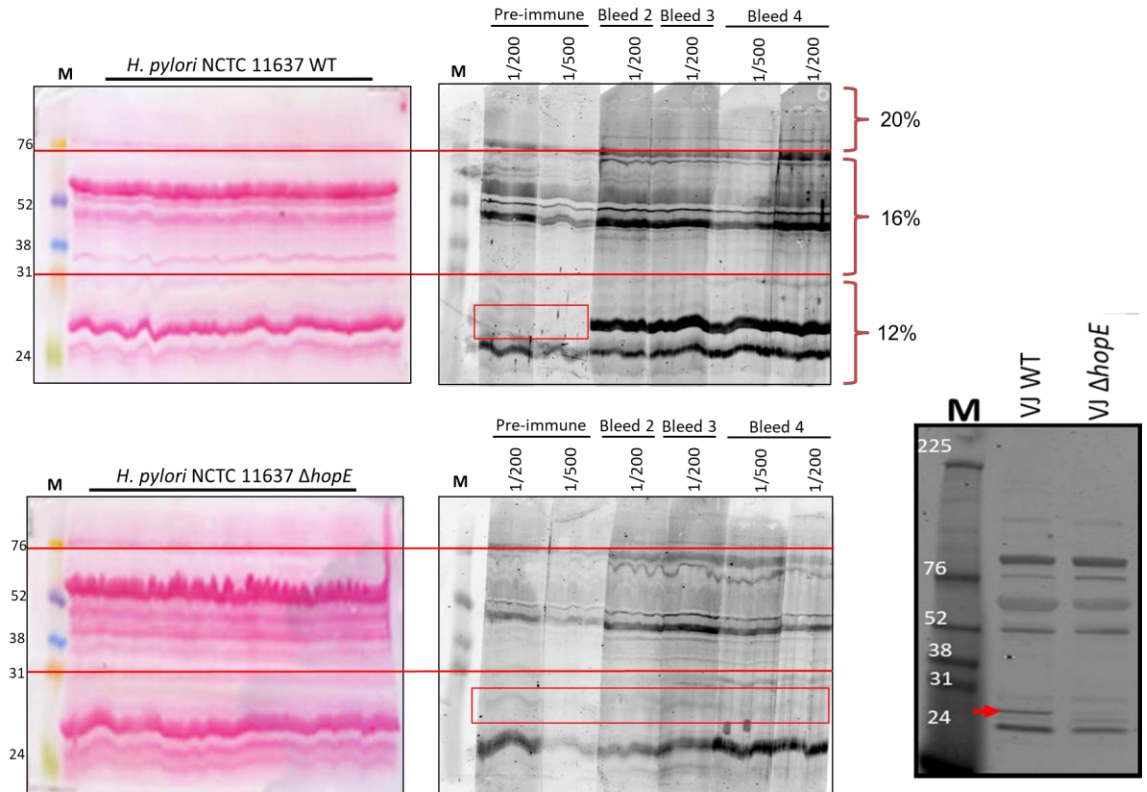
Figure 7. Optimizing the anti-HopE antibodies for Western blotting.

The bacterial cells were lysed by mechanical disruption and the OM components were separated via ultracentrifugation. Western blotting was performed on OM samples using anti-HopE antibodies. The red horizontal lines mean the demarcation of transition from 20-16% and 16-12% acrylamide (the gel layout is shown at the top right). Left pink blots are due to Ponceaus S red staining of proteins. The nitrocellulose membrane was cut into strips and incubated separately according to the serum bleed and concentration. Red box = protein band ~27 kDa that is non-reactive to pre-immune in WT and both pre-immune and all bleeds in the *hopE* knockout mutant. The bottom right image depicts the current final application of the anti-HopE Western blotting; red arrow denotes the location of the HopE band. M = molecular weight marker.

The red box in Figure 7 denotes a protein band smaller than 30 kDa that is not reactive in the pre-immune stage but reactive in the bleeds in WT. This protein is also not present in the *hopE* mutant blot. The bleed that was chosen to perform further anti-HopE Western blotting was from the final bleed (bleed 4) at a concentration of 1/200. Based on these experiments, HopE could be reliably detected using the optimized anti-HopE Western blot conditions.

A vast number of protein bands were also reactive to these new HopE antibodies. Thus, we investigated the reason behind this by comparing the peptide sequence used to raise the antibodies against the OM proteins (OMPs) of HP. To date, we have compiled a list (Figure 8) of OMP sequences that was obtained by blasting HopE against the HP genome using the NCBI protein BLAST online tool. The results indicated that our peptide sequence that we used for rabbit immunization (GYKKFFQFKSLDMTS) is found in many OMPs, although with varying levels of conservation. However, this may not be the cause of the cross-reactivity, as the naïve pre-immunized serum also has this similar pattern of cross-reactivity (Figure 7). Nevertheless, the cause of this phenomenon was not pursed further because these bands do not prevent us from detecting our protein of interest.

```
epitope        GYKKFFQFKSLDMTS
 HP0706    LNVGYKKFFQFKSFDMTSK
 HP0009    VQIGYKQFFGEKRRWGLRY
 HP1177    VQVGYKQFFGEKKRWGLRY
 HP0722    VQVGYKQFFGESKRWGLRY
 HP0725    VQVGYKQFFGESKRWGLRY
 HP1342    VQVGYKQFFGKKRNWGLRY
 HP0227    VQVGYKQFFGKKRNWGLRY
 HP0896    IQVGYKQFFGQKRKWGARY
 HP1243    IQVGYKQFFGQKRKWGARY
 HP0317    IQVGYKQFFGQKRKWGARY
 HP0025    FQVGYKQFFGKNKRWGARY
 HP1156    VKMGYKQFFGKKRMFGLRY
 HP0229    VQLGYKQFFGKNKFFGIRY
 HP0671    LTVGYKQFFGEKRWFGARY
 HP1469    FEVGYKQFFGKKKWFGMRY
 HP1501    VMTGYKHFIGKKRWFGLRY
 HP0477    LSVGYKHFFTKKKNQGLRY
 HP0923    LSVGYKHFFTKKKNQGLRY
 HP0912    TKIGYKQFFGKKRNIGLRY
 HP0913    TKIGYKQFFGENKNVGLRY
 HP0252    AKMGYKQFFTHKKNVGLRY
 HP0127    FVVGYKHFFKKSPQFGMRY
 HP0796    LIYGYKQFFPKKERYGFRF
 HP0079    AMAGYKWFFGKTKRFGFRS
 HP0638    LSFGYKYFLGKKRIIGFRH
 HP1157     GLGYKYFFGKARKLGLRHV
 HP0324    LVMGYNHFFHPDKILGLRY
 HP1395    ALLGYQFFFGK--YFGLRLVG
 HP1113    VQVGYKWVGKHEETKWFGF
Consensus  ...GYk.Ffgkk...g.ry.
```

Figure 8. Complete list of OMPs that have similarities to the HopE epitope.
The green highlighted box indicates the location within the 28 non-HopE outer membrane protein sequences that have a high degree of consensus with the HopE epitope. The red amino acids are found within all the genes at that location, while the blue amino acids are found within the majority of the genes at that location.

3.2   All strains generated for this study

3.2.1   Initial strains available in the lab and problems encountered

Some of the original strains that had been ready for preliminary investigation were a WT and a Δ*hopE* mutant derived from this WT, labelled Maryam Khodai (MK) WT and Brandon Oickle (BO) Δ*hopE* mutant, respectively. Due to the repeated passages of MK WT separate from its Δ*hopE* mutant, we could not be certain that the pair remained isogenic. It was possible that because the WT was carried independently, phase variation might have occurred, which concerns the LPS synthesis fucosyltransferase genes. In order to standardize the Western blot and antibiotic testing results, the LPS patterns of all the strains must be taken into account as they matter greatly when interpreting the results of antibiotic sensitivity assays presented later, since the LPS can play a role as a barrier to prevent intake of the antibiotic. Additionally, the LPS can also cause interference in identifying Lewis Y or BambL reactive proteins and diminish the observation of phenotypes that relate to proteins on the surface of the cell. Therefore, finding or creating closely matching strains in terms of LPS patterns is important to isolate phenotypes specifically due to HopE.

3.2.2   Generation of mutants relevant to this study

Rationale for VJ Δ*hopE*:

Since the MK WT had been passaged repeatedly by other lab members and may suffer from phase variation that alters surface properties, the VJ Δ*hopE* was generated during this thesis work using VJ WT as the recipient (Figure 9), therefore producing an isogenic pair.

Results for VJ Δ*hopE*:

Transformation of the *hopE* knockout construct into the VJ WT strain resulted in the production of 4 clones (Figure 9). Screening these clones via PCR and DNA sequencing   indicated   that   several   clones   had   successfully   incorporated   the

chloramphenicol resistance (CAT) cassette into the *hopE* gene, producing VJ Δ*hopE*. Clone #2 was chosen to be the isogenic pair to VJ WT and its outer membrane was extracted for subsequent analysis.

+ CAT = 1618 bp
- CAT = 1463 bp
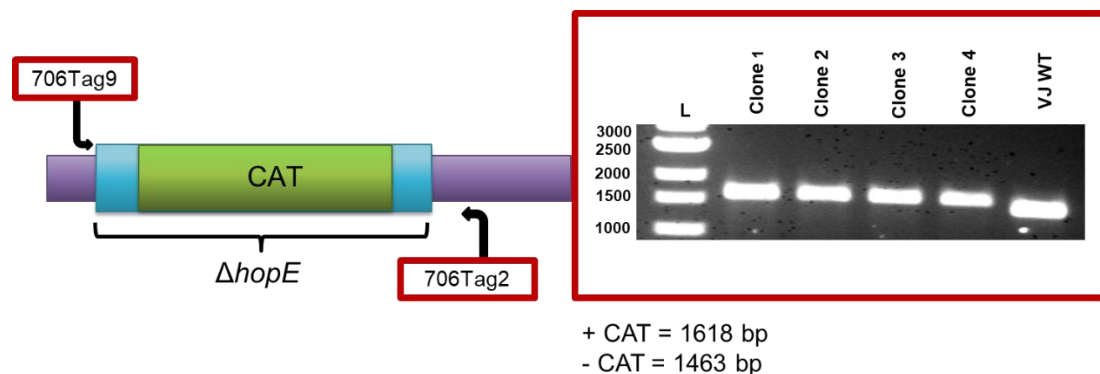
Figure 9. Creation of VJ Δ*hopE*.

The location of primers used for the analysis is shown in the schematic next to the gel results. Succesful insertion of the *hopE* knockout construct was verified by the presence of the *hopE* chloramphenical (CAT) resistance cassette (size of this PCR product would be 1618 bp). Wild-type control without the cassette in *hopE* (- CAT) had a PCR product size of 1463 bp. L = molecular weight standards.

Rationale for Δ*hopE*/Δ*waaL*:

To better visualize the HopE protein and its potential Lewis glycosylation in absence of LPS, we created the double knockout mutant Δ*hopE*/Δ*waaL* by inserting the *hopE* knockout construct into the Δ*waaL* strain through natural transformation (Figure 10). With the O-antigen ligase function knocked out, there would be no fully formed LPS structure although O-units of Lewis Y antigens would still be formed. Thus, it should have no LPS-based Lewis Y reactivity while any glycoprotein-based reactivity would be present during Western blotting. Additionally, this double knockout mutant would also provide information on the function of HopE during assays to investigate its role, as

removal of the LPS may provide greater access to the porin on the outer membrane. This double knockout mutant would be compared to the reference strains Δ*waaL* and Δ*hopE* and is isogenic to Δ*waaL*.

One caveat to mention is that if WaaL is responsible for HopE glycosylation by transferring the Lewis Y onto HopE, then this double knockout mutant would not show any difference of Lewis Y reactivity when compared to the single Δ*waaL* mutant. However, according to our hypothesis, the OST is not WaaL but is HP0946. We still carried out systematic studies using the WT WaaL strains to ascertain if WaaL was involved (Figure 10).

Results for Δ*hopE*/Δ*waaL*:

Performing the transformation of Δ*hopE*/Δ*waaL* resulted in the generation of 20 clones (Figure 10). The first ten were screened by PCR and their chromosomal DNA was extracted. The resulting screening and DNA sequencing indicated that several clones had successfully incorporated the chloramphenicol resistance (CAT) cassette into the *hopE* gene and of these, clone #10 was selected for downstream applications. As such, we proceeded to extract the outer membranes of this double knockout mutant clone.
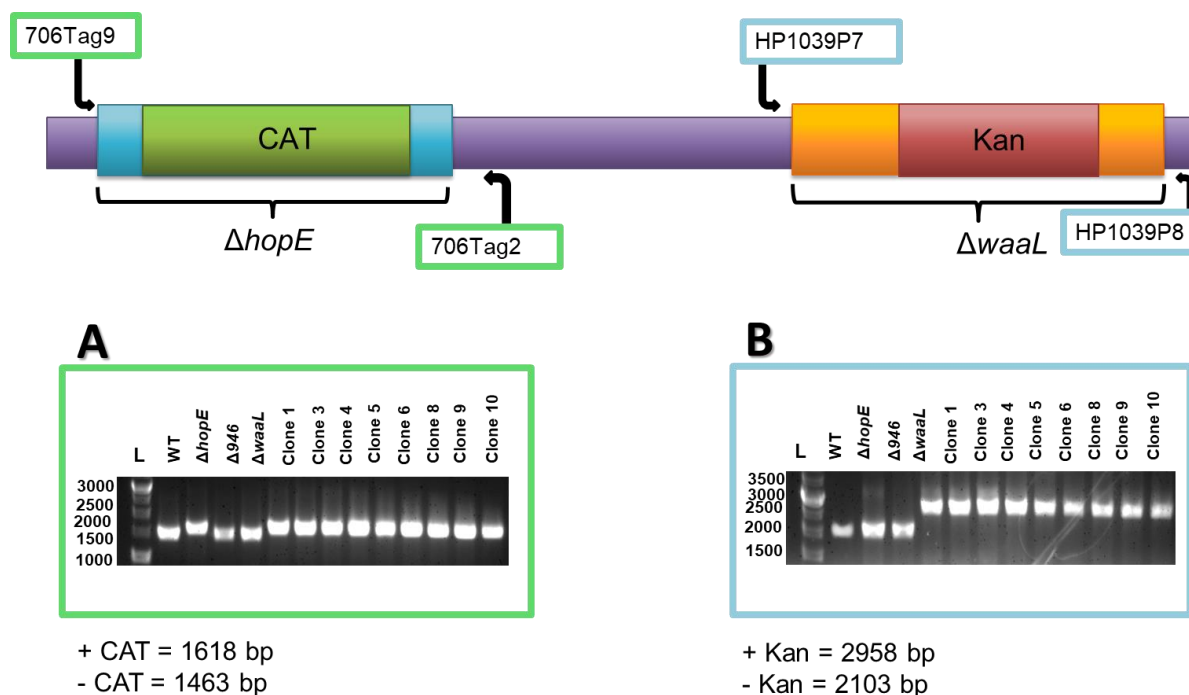
Figure 10. Generation of Δ*waaL*/Δ*hopE* and the resulting PCR analysis.
The location of primers used for the analysis is shown in the schematic above the corresponding DNA gels. A) The presence of the *hopE* chloramphenical (CAT) resistance cassette increased size of the PCR product to 1618 bp. Lack of the cassette resulted in a product of 1463 bp. B) Clones with the kanamycin (Kan) resistance cassette in the correct location had a product size of 2958 bp. Strains without the kanamycin cassette in *waaL* had a PCR product size of 2103 bp. L = molecular weight standards.

Rationale for Δ*hopE*/Δ*946*:

According to anti-Lewis Y and BambL Western blots (shown later, Figures 14 and 17), the LPS patterns of the WTs did not correspond well to the LPS patterns of the Δ*hopE* mutants or the Δ*946* mutant. This renders an accurate comparison between the WT and the mutants difficult, as several of the assays performed in my project may be affected by the composition/arrangement of the LPS pattern. However, the Δ*hopE* mutants and the Δ*946* mutant have similar LPS patterns (they have more abundant lower molecular weight LPS molecules than the WTs in the anti-Lewis Y blots), thus it would

be desirable to make a double knockout mutant using the Δ*946* strain as the backbone in which to incorporate the Δ*hopE* construct. In this manner, the double knockout mutant can be compared to its respective single knockout mutants, using them as the reference instead of the WTs which do not have a matching LPS pattern. Unlike the Δ*hopE/ΔwaaL* double knockout mutant which does not have functional LPS pattern, this double knockout mutant will still have LPS O-antigen and is isogenic to Δ*946* (Figure 11).

Results for Δ*hopE*/Δ*946*:

After the transformation of Δ*hopE*/Δ*946*, 9 clones were obtained and their chromosomal DNA was extracted and screened by PCR. All the tested clones showed a PCR band consistent with the expected size. However, since the difference between the clones and the controls without the CAT cassette are minimal and could not be resolved on the agarose gel, DNA sequencing was performed. DNA sequencing indicated that several clones had successfully incorporated the chloramphenicol resistance (CAT) cassette into the *hopE* gene (Figure 11) and of these, clone #6 and #7 were selected for antibiotic assays. Additionally, the outer membrane was extracted from this double knockout mutant clone #7 and Western blots and silver staining (with Proteinase K treatment) was performed.

706Tag9

CAT

Kan

ΔhopE

706Tag2

Δ946

+ CAT = 1618 bp
- CAT = 1463 bp
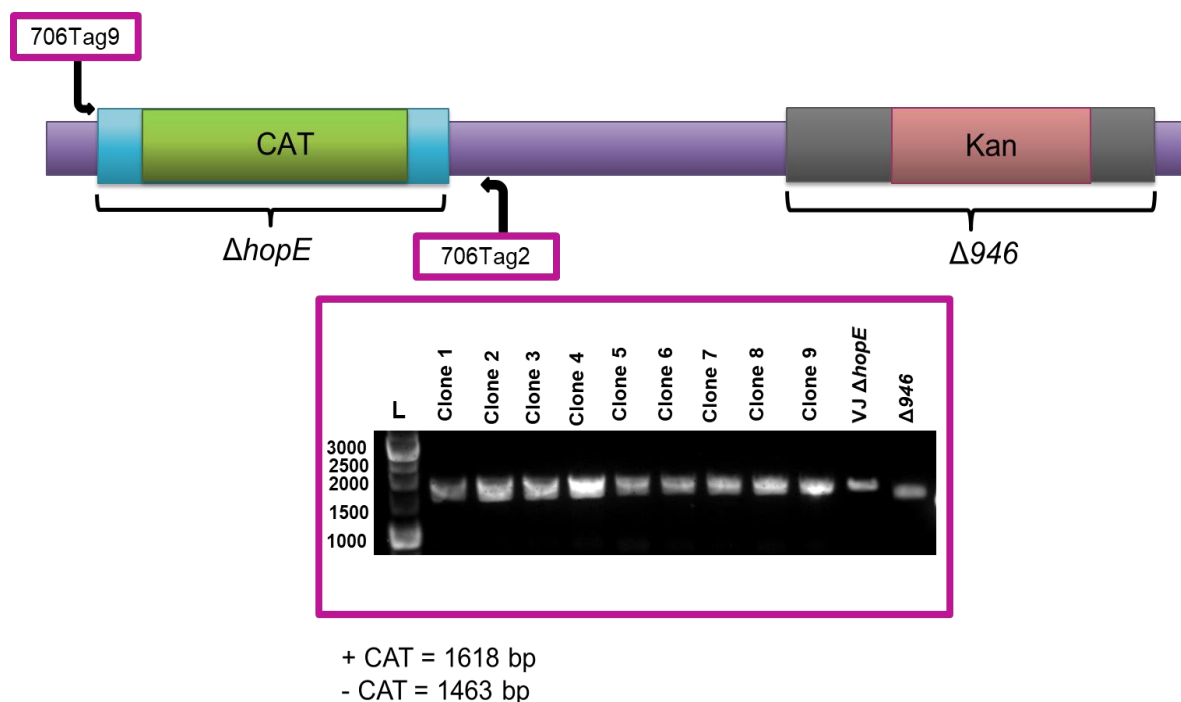
Figure 11. Creation of the Δ*hopE*/Δ*946* double knockout mutant and the resulting PCR analysis.

The location of all primers is shown in the schematic above the gel result. Presence of the *hopE* chloramphenical (CAT) resistance cassette in *hopE* is indicated by the PCR product size of 1618 bp. Absence of the CAT cassette in *hopE* is indicated by the product size of 1463 bp. The Δ*hopE* construct was transformed into the Δ*946* mutant that had been previously verified by another lab mate, Justine Denomme. L = molecular weight standards.

3.2.3 PCR analysis of the LPS synthesis-related genes for phase variation

Rationale:

In addition to ensuring that the various strains had the proper sequence in the genes of interest, the fucosyltransferases FutA and FutC and the Wzk flippase genes underwent PCR and sequencing analysis. The fucosyltransferases are enzymes required for the production of Lewis antigens, as well as LPS chain length regulation and have

highly phase variable regions in their genes[31]. The Wzk enzyme, while not phase variable, is the flippase that transfers the O polysaccharide unit to the periplasm, where the WaaL O antigen ligase attaches it to the lipid A core[23]. Thus, changes to these genes could significantly affect the LPS structure of the bacteria, possibly resulting in phenotypic changes such as a change in antibiotic susceptibility. However, the fucosyltransferases are not the only genes with homopolymeric tracts that may potentially inactivate their function. In fact, there are a total of 27 phase variable genes in all of HP[72].

Results:

Analysis of the FutA, FutC and Wzk genes show no difference between the FutA and Wzk sequences of all the strains; the enzymes were all in frame and therefore should be functioning properly. The FutC gene was not in frame for most of the strains, indicating that the full protein is likely not formed. However, it is likely that a truncated form of FutC is still functioning, since the strains capable of making O-antigens are still producing bands that react to Lewis Y (seen in anti-Lewis Y Western blotting). As FutC is the only known enzyme in the LPS synthesis pathway that can create the Lewis Y motif (see Figure 4), it is possible that since frame shifting occurs after the motif I, this may be enough to perform the catalytic function of attaching the terminal fucose.

3.2.4   Analysis of the LPS of working *H. pylori* strains

Rationale:

In order to determine the LPS pattern of the various strains, samples were treated with Proteinase K (PK) and subjected to silver staining. This procedure should eliminate protein signals and allow the observation of each strain's LPS profile. Additionally, it could identify potential LPS present in the silver stain that is neither Lewis Y nor BambL reactive. Sample loading was reduced as silver staining is a highly sensitive method that does not require the same volume of sample input as the Western blots do.

Although the OM preparations were made from normalized samples of the HP strains (same optical density during harvest, same volumes used during OM extraction), the volume of sample to use for these gels were refined using the Ponceau S stains of Western blots to ensure that all the samples were loaded equally according to protein content. Concurrently, a Coomassie stain to detect proteins was also performed with the same samples to identify any proteins that may not have degraded completely during the PK treatment and might be mistaken for LPS in the silver stain. Additionally, to identify LPS patterns using anti-Lewis Y and BambL, the OM samples were digested with Proteinase K and their LPS was detected via Western blotting.

Results:

The silver staining results (Figure 12A) showed that the Δ*hopE* and Δ*946* mutants had higher molecular weight silver-reactive bands (~31 – 40 kDa, indicated by a green bracket), that are either undigested proteins or LPS. According to the Coomassie stain, these bands are not proteins that were resistant to digestion as there is no Coomassie reactivity in that area, thus they are likely LPS molecules. However, this silver response was not seen in the WTs and Δ*waaL* and Δ*hopE/ΔwaaL* double knockout mutant. As the Δ*waaL* and Δ*hopE/ΔwaaL* mutants do not have a functional O-antigen ligase, the lack of this LPS is understandable. This is not as easily explained in the WT strains; the two WT strains also had less lipid-A core than the other mutants. Thus, it is possible that despite our best efforts at calculating to aim for equal loading, WT samples were loaded less than the other strains. To determine if this was the case, silver staining was performed again on new samples.

According to Figure 12B, the O-antigen products of the newly prepared OM sample of the VJ WT strain was clearly visible unlike in Figure 12A. This indicated that despite obtaining OM samples for all strains at similar optical densities with no changes in the extracting of the OM component, there was still variations in the silver stain response. It appears that OM samples weren't precisely reproducible due to the likelihood of variable O-antigen expression. The variation of HP's O-antigen expression could also affect antibiotic assays as the LPS plays a crucial role in repelling antibiotics. Thus, it

was essential to perform 3 independent biological replicates for all antibiotics assays conducted in this thesis. Figure 12B also provides a comparison of the newly extracted Δ*hopE*/Δ*946* double knockout mutant with its isogenic Δ*946* mutant. No difference in this LPS pattern was seen, as expected and antibiotic assays can be performed and compared between these two strains and Δ*hopE* faithfully. Overall, Δ*hopE* does not change the LPS pattern when comparisons are made with the properly matched isogenic strains.
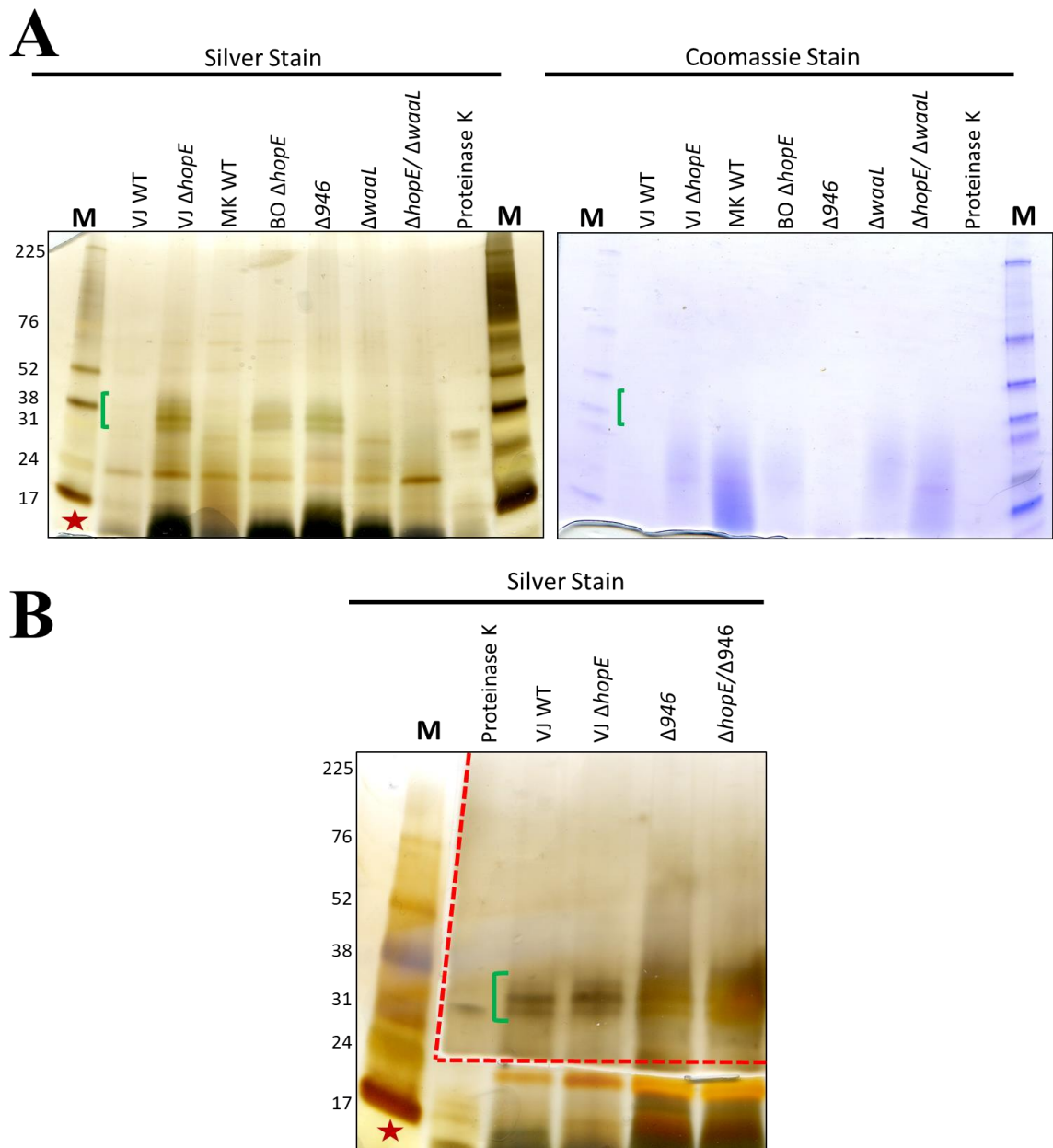
Figure 12. Silver and Coomassie staining of Proteinase K treated samples.
OM samples were subjected to Proteinase K (PK) treatment and subsequently run on
BioRad precast gradient gels, 4-20%. A) One gel was developed with silver (left) and the
other with Coomassie (right). B) After staining the lipid-A core, the gel was cut along the
red dashed lines and re-stained with silver to expose the higher molecular weight bands.
Location of the LPS O-antigen is seen with the green bracket. Red star indicates location
of the lipid-A core. M = molecular weight markers.

Results of the anti-Lewis Y and BambL blots showed the different LPS pattern between the two WTs, making it clear that MK WT's LPS profile appears to have been altered in some way. This does not mirror the results of the silver stain, causing a paradox. Silver staining is reportedly very sensitive, which is why less OM samples are to be used when staining them with silver since they react so strongly. However, it is very evident when comparing Figures 12 and 13 that the silver stain could not pick up the higher molecular weight bands (greater than 40 kDa) seen using anti-Lewis Y antibodies and BambL lectin. The reason for this was not investigated further at this point, especially since MK WT had proved not to be isogenic to the BO Δ*hopE* mutant.
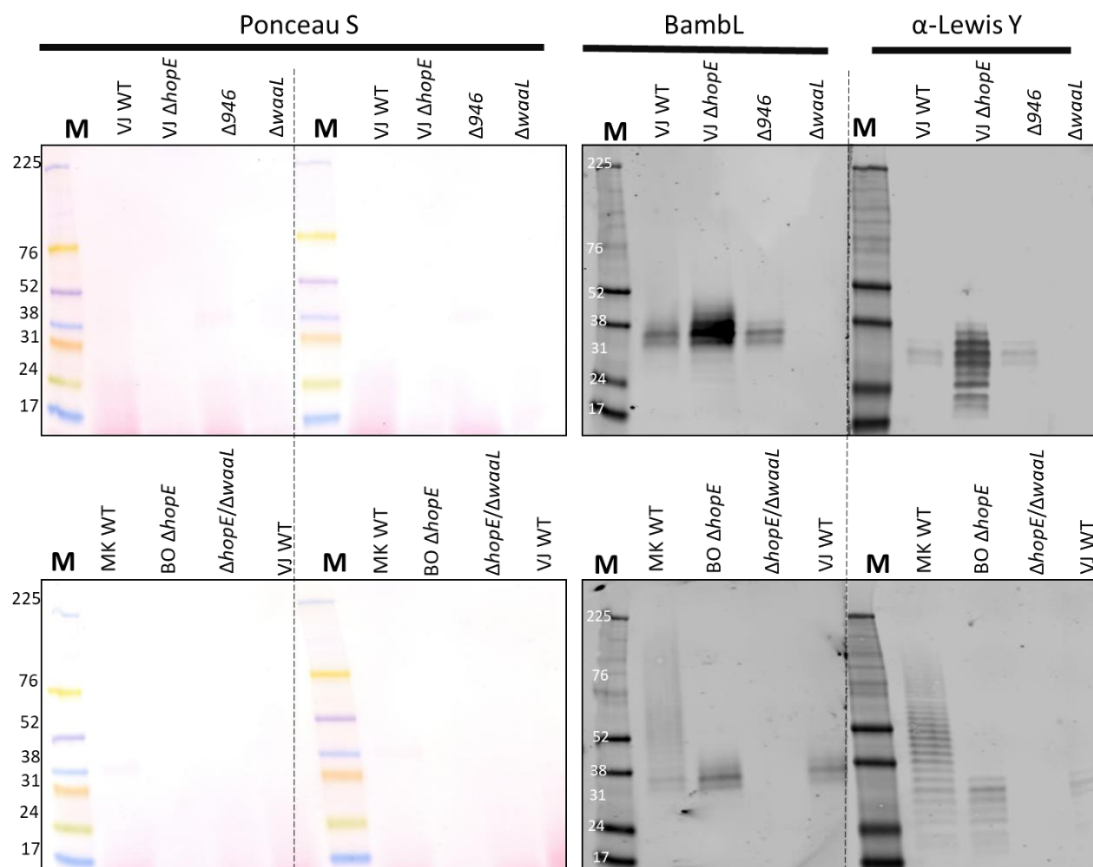
Figure 13. Visualizing the LPS pattern via anti-Lewis Y and BambL Western blotting of PK treated OM samples.

OM samples were subjected to Proteinase K (PK) treatment and subsequently run on BioRad precast gradient gels, 4-20%. The membranes were cut in half, one-half incubated for anti-Lewis Y blotting and the other half for BambL blotting. Membranes were also stained with Ponceau to visualize any undigested proteins. M = molecular weight markers.

3.2.5   Analyzed characteristics of the working *H. pylori* strains

During the course of this thesis, the relevant characteristics of the working strains were consolidated into a table (Table 3). The working strains used were VJ WT, MK WT, VJ Δ*hopE*, BO Δ*hopE*, Δ*946*, Δ*waaL*, Δ*hopE*/Δ*waaL*, and Δ*hopE*/Δ*946*. As the table illustrates, there appears to be no difference in the silver stain LPS pattern for isogenic

strains with a functional *waaL* gene. However, there does appear to be differences in the LPS pattern when visualized using PK treated samples in anti-Lewis Y and BambL blots (Figure 13). To understand the reasoning behind this phenomenon, the fucosyltransferases FutA and FutC and the Wzk flippase were analyzed via PCR. Sequence analysis of the fucosyltransferase PCR products indicated that there were no differences between the gene sequences of these strains that could explain the LPS variation. Likely, this LPS variation is a consequence of other genes such as the remaining 25 phase variable genes. It does appear that most genes do not have an "in-frame" FutC gene. However, since the strains are reacting to the Lewis Y antibodies, it is likely that the FutC gene is still functional by virtue of its most N-terminal transferase domain that is in frame. Although Δ*hopE/*Δ*waaL*'s FutC is in-frame, the deletion of the *waaL* gene prevents LPS from being incorporated onto the outer membrane, thus it is not relevant that FutC's sequence in Δ*hopE/*Δ*waaL* is different from the other strains since the LPS result of FutC being in frame would not be observed. However, it is relevant in terms of the nature of the O-antigen units that can be made and are available for glycosylation.

Table 3. List of features that have been analyzed for all working strains.

Strain	LPS O-antigen (Silver stain)	LPS O-antigen (Lewis Y/ BambL)	Resistance Cassette	PCR of Fut A	PCR of Fut C	PCR of Wzk
VJ WT	Short (~31-40 kDa)	Short (~31-40 kDa)	---	In-frame gene	Gene is not in frame and the full protein is likely not formed.	In-frame gene
VJ ΔhopE	Short (~31-40 kDa)	Long (~20-40 kDa)	Chloramphenicol	In-frame gene	Gene is not in frame.	In-frame gene
MK WT	Short (~31-40 kDa)	Long (~20-100 kDa)	---	In-frame gene	Gene is not in frame.	In-frame gene
BO ΔhopE	Short (~31-40 kDa)	Long (~20-40 kDa)	Chloramphenicol	In-frame gene	Gene is not in frame.	In-frame gene
Δ946	Short (~31-40 kDa)	Short (~31-40 kDa)	Kanamycin	In-frame gene	Gene is not in frame.	In-frame gene
ΔhopE/ Δ946	Short (~31-40 kDa)	TBD	Chloramphenicol and kanamycin	In-frame gene	Gene is not in frame.	In-frame gene
ΔwaaL	Absent	Absent	Kanamycin	In-frame gene	Gene is not in frame.	In-frame gene
ΔhopE/ ΔwaaL	Absent	Absent	Chloramphenicol and kanamycin	In-frame gene	In-frame gene	In-frame gene

"Gene is not in frame" signifies that the strain is missing a 15th C base in the homopolyC tract of FutC that would render the gene "in-frame".

3.3 Investigating HopE glycosylation with anti-Lewis Y

Rationale:

To determine the possibility of HopE glycosylation, the OM samples of several of the strains were extracted and run on commercially produced precast 4-20% gradient gels. These gels are the same as those used for LPS analyses described above in section 3.2 and were utilized to replace the home-made step-wise gels shown in Figure 7 in an attempt to obtain more reproducible Western blots and defined protein/LPS bands to allow for easier comparison between samples in a single blot and between two or more different blots. Additionally, the use of these gradient gels may also allow easier resolution of the HopE band away from the Lewis Y reactive LPS bands. When performing this Western blot, half of the membrane was blotted with anti-HopE antibodies while the other half was blotted with anti-Lewis Y antibodies.

Results:

In Figure 14A, comparing the lanes with strains containing HopE indicated by the red arrows (VJ WT, MK WT, Δ*946*, Δ*waaL*) to those with the *hopE* gene knocked out, anti-Lewis Y signal intensity does not change (bottom panel) or even increases (top panel). If HopE was truly glycosylated by a Lewis motif, the elimination of HopE should result in a notable decrease in anti-Lewis Y signal in the Δ*hopE* mutants. This indicates that HopE may not be glycosylated with Lewis Y. Additionally, the Lewis Y signal is still present in the Δ*hopE*/Δ*waaL* mutant in the HopE region, further indicating that HopE is not glycosylated by Lewis Y. However, presence of Lewis Y reactive bands in the Δ*hopE*/Δ*waaL* and Δ*waaL* mutants suggest the possible presence of other Lewis Y glycosylated proteins, since the LPS O-antigen is eliminated from these two mutants.

In Figure 14B, the Western blots in Figure 14A were manipulated in Photoshop by inverting the colours that appear when scanning the membrane (red wavelength became blue, green wavelength became pink) to provide better visualization when these blots were overlayed on top of each other. This analysis was performed to provide more

proof of the possible lack of Lewis Y HopE glycosylation. If an anti-HopE reactive band was also reacting to anti-Lewis Y, the band would show as purple.

However, these overlays did not work as well as they could have, due to differences of migration of the samples in the lanes for the anti-HopE blot versus the lanes for the anti-Lewis Y blot in the left panel. The VJ WT and the Δ*waaL* lanes experienced a slight lane distortion upward in the anti-Lewis Y blot but downward in the anti-HopE blot, making it impossible to overlay the bands. In this blot, we can only accurately compare the overlays of the middle two lanes (VJ Δ*hopE* and Δ*946*) as the samples did not distort in either the anti-HopE or anti-Lewis Y blots. Therefore, the HopE band in Δ*946* coincides with a Lewis Y band, but that band is still present in the VJ Δ*hopE* mutant, thus it is likely that the Lewis Y signal is not due to HopE glycosylation. For the right-side panel, very little distortion was observed, making overlaying the two blots possible. As there is still a blue Lewis Y reactive band in this Δ*hopE* mutant, these inverted blots have the potential to provide further evidence that the Lewis Y reactive band is not HopE.

Interestingly in the anti-Lewis Y Western blot, the Δ*946* mutant exhibits a Lewis Y pattern that is entirely different than the other strains. As the function of HP0946 is unknown, complementation of this protein could confirm whether this altered Lewis Y pattern is a product of eliminating HP0946. However, this was not attempted yet due to time constraints.

To determine the specificity of the anti-HopE and anti-Lewis Y Western blot results, blotting half the membranes with only secondary antibodies (Figure 15 and 16, "-primary") showed that the secondary goat anti-rabbit antibodies (that bind to anti-HopE antibodies) and the secondary goat anti-mouse antibodies (that bind to anti-Lewis Y antibodies) elicited very little cross-reactivity. The results of Figure 15 implied that there is low non-specific binding by the secondary antibody. Similarly, the results of Figure 16 also indicated that the anti-Lewis Y Western blotting membranes blotted with both antibodies were very specific and is likely only reacting with bands that contain Lewis Y antigens.
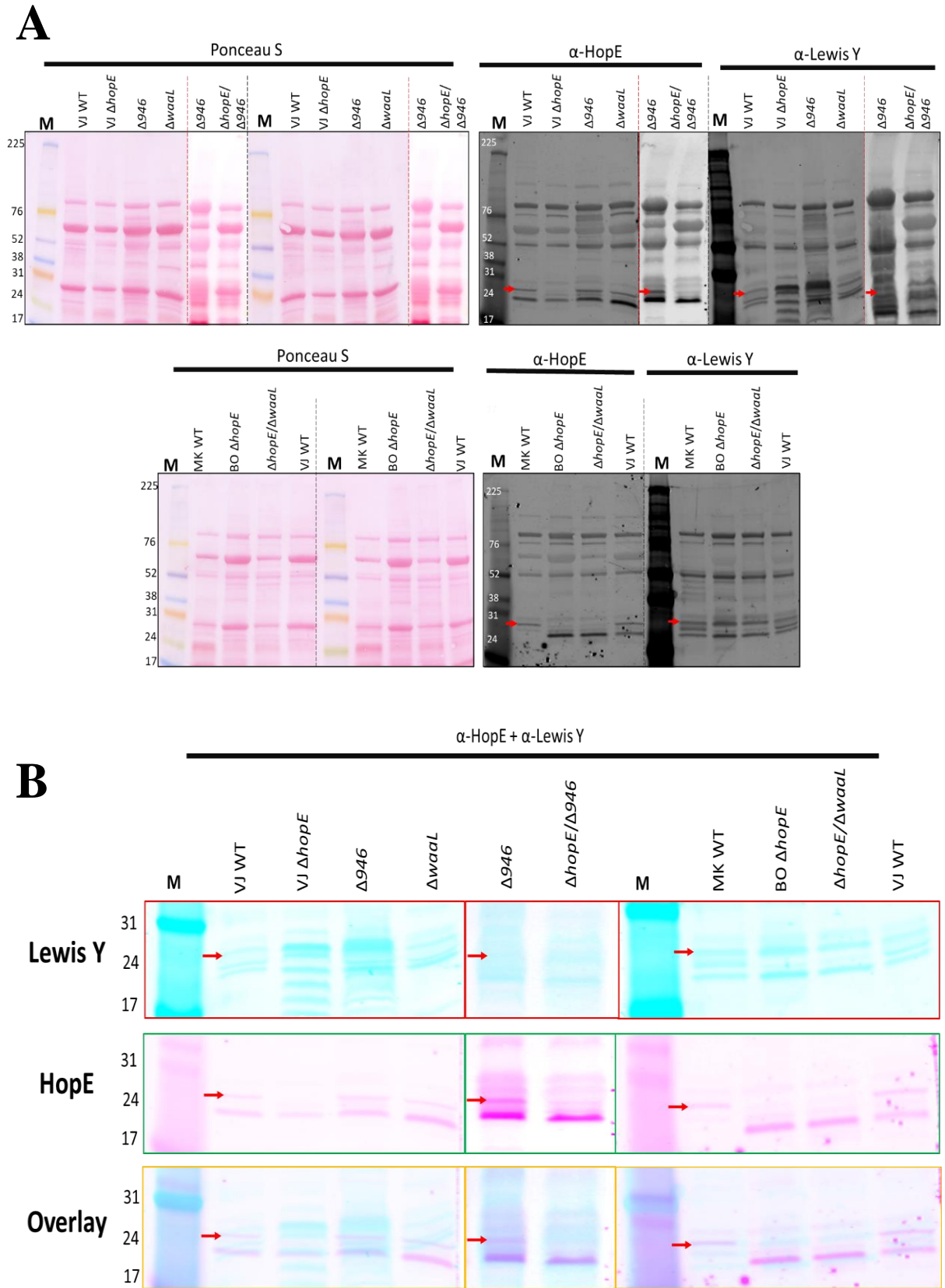
Figure 14. Ponceau S stain and Western blot to investigate HopE glycosylation by Lewis Y.

A) Western blot of OM preparations detected with anti-HopE and anti-Lewis Y antibodies on precast gradient gels (4-20%). Ponceau S stained membranes are shown on the left to visualize proteins. The red dashed lines indicate that the Δ*hopE* and Δ*hopE*/Δ*946* mutants shown together were run on different gels at a later date to the rest of the blot. Alignments were performed based on the molecular weight marker locations and overlaying blots and matching the markers on both blots to each other. Sometimes, non-specifically reacting protein bands on both blots are also aligned. Alignment via this method is not always absolute as there are two separate membranes being used in which warping can occur. B) Enhanced view of the two blots. The blots were inverted to obtain the pink and blue colours using Photoshop in order to better visualize the bands when they are overlayed on top of each other. The red arrow indicates the location of the HopE band. M = molecular weight markers.

Figure 15. Ponceau S staining and anti-HopE Western blot of OM samples to determine antibody specificity.

Western blot of OM samples on gradient gels (4-20%), detected with freshly made anti-HopE primary and secondary antibodies. Ponceau S stained membranes are shown on the right to visualize proteins. M = molecular weight markers.
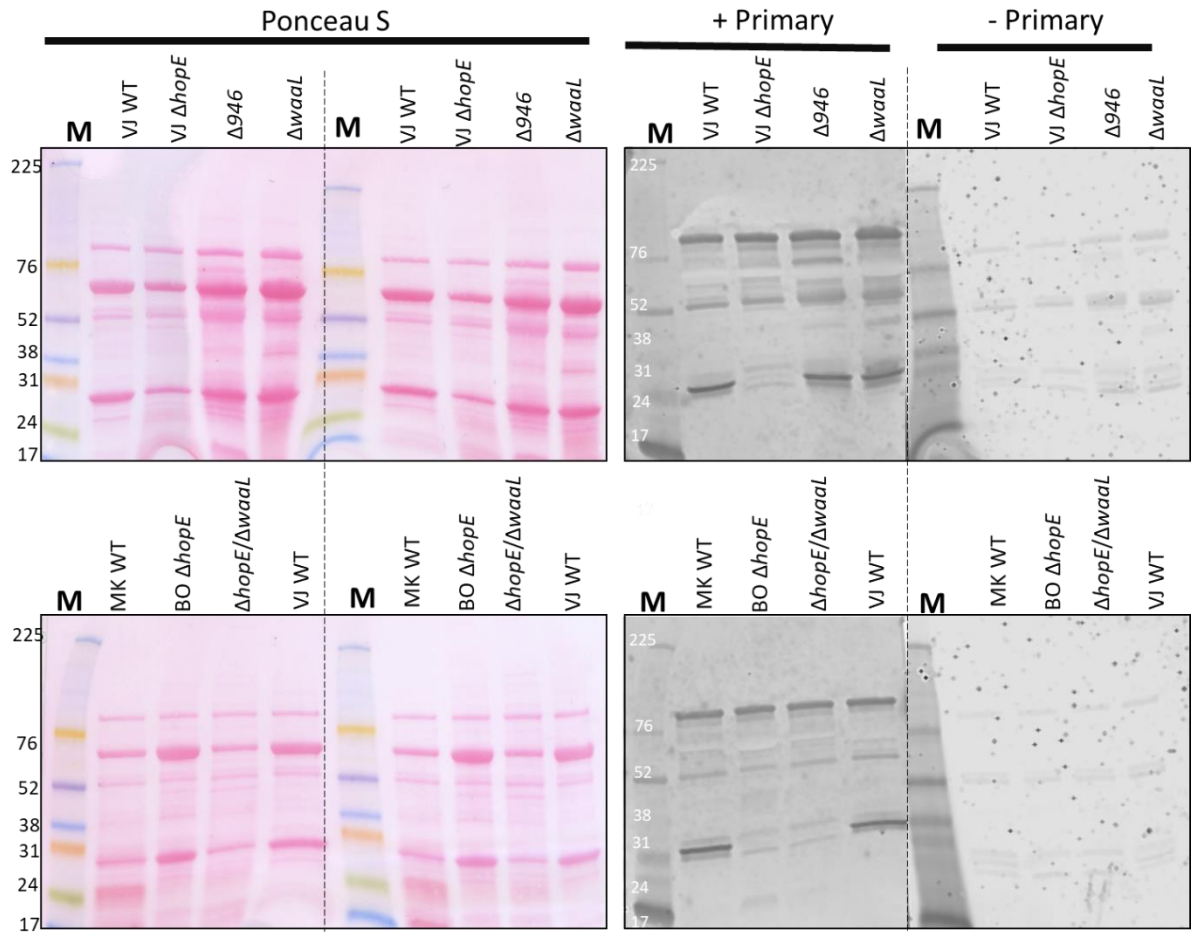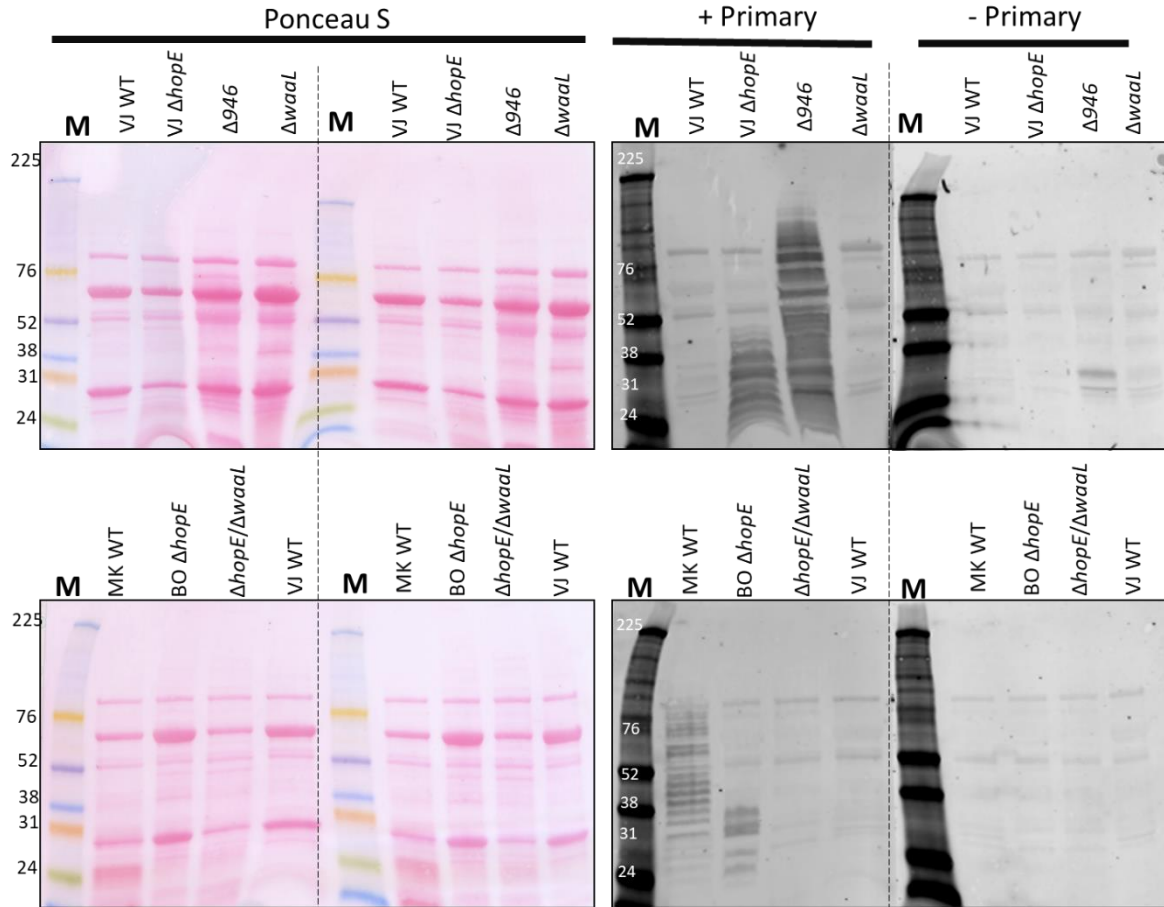
Figure 16. Ponceau S staining and anti-Lewis Y Western blotting of OM samples to determine antibody specificity.

Western blot of OM samples on gradient gels (4-20%), detected with freshly made anti-Lewis Y primary and secondary antibodies. Ponceau S stained membranes are shown on the left to visualize proteins. M = molecular weight markers.

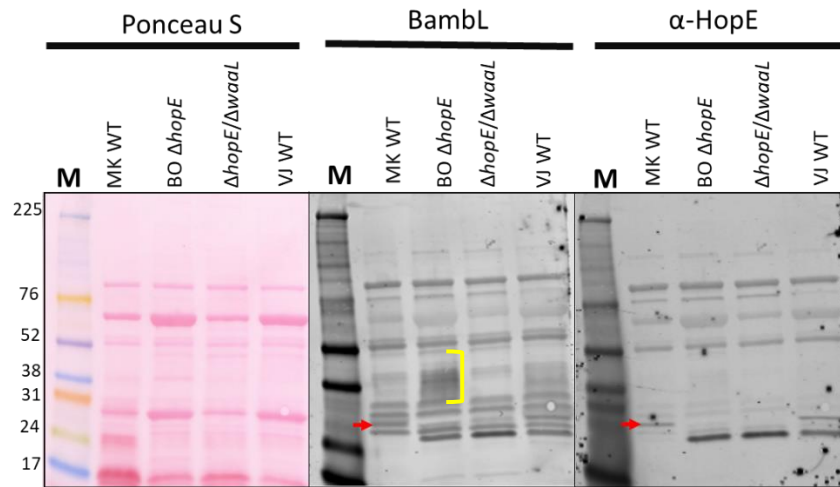## 3.4   Investigating HopE glycosylation with lectin BambL

Rationale:

Although HopE is likely not glycosylated by Lewis Y, this does not eliminate the possibility that HopE is glycosylated with a non-Lewis Y glycan. To investigate this possibility, a Western blot was performed with fucose binding biotinylated lectin BambL and fluorescently labelled streptavidin. After blotting half of the membrane with this BambL the blot was re-probed with anti-HopE antibodies to determine the location of HopE; this strategy allows direct overlay of both blots. The original blots and enhanced blots are shown in Figure 17.

Results:

Comparing the isogenic strains containing HopE in Figure 17 to the strains without it (HopE is indicated by the red arrows), the BambL reactive band appears to be lost when the porin expression is eliminated in the *hopE* knockout mutants. This is particularly apparent on the blot overlays. Thus, HopE may be glycosylated by another fucose carrying glycan.

Interestingly, removal of the HopE protein results in increased generation of higher molecular weight fucose-containing bands (that are reactive with BambL) not seen in the WT strains (indicated by the yellow brackets). The generation of higher molecular weight BambL reactive bands is enhanced even more when eliminating the HP0946 protein, whose function is still unknown. Indeed, this phenotype is also seen in the double knockout mutant Δ*hopE*/Δ*946*. It is likely that within the Δ*946* mutant, the higher molecular weight bands are Lewis Y O-antigens, as this BambL pattern is present in the Lewis Y Western blots as well. Additionally, there is still BambL reactivity within the HopE area for the Δ*946* mutant, which is confirmed when comparing to the WT, Δ*hopE* mutant and Δ*hopE*/Δ*946* mutant. providing evidence that HP0946 may not be the OST for HopE glycosylation. BambL reactivity also appears to be conserved in the Δ*waaL* mutant, therefore WaaL would also not be responsible for HopE glycosylation by the BambL reactive motif.

According to Figure 18, observing the BambL + streptavidin blots against the streptavidin only blots shows there is very little non-specific binding occurring due to incubation with streptavidin.
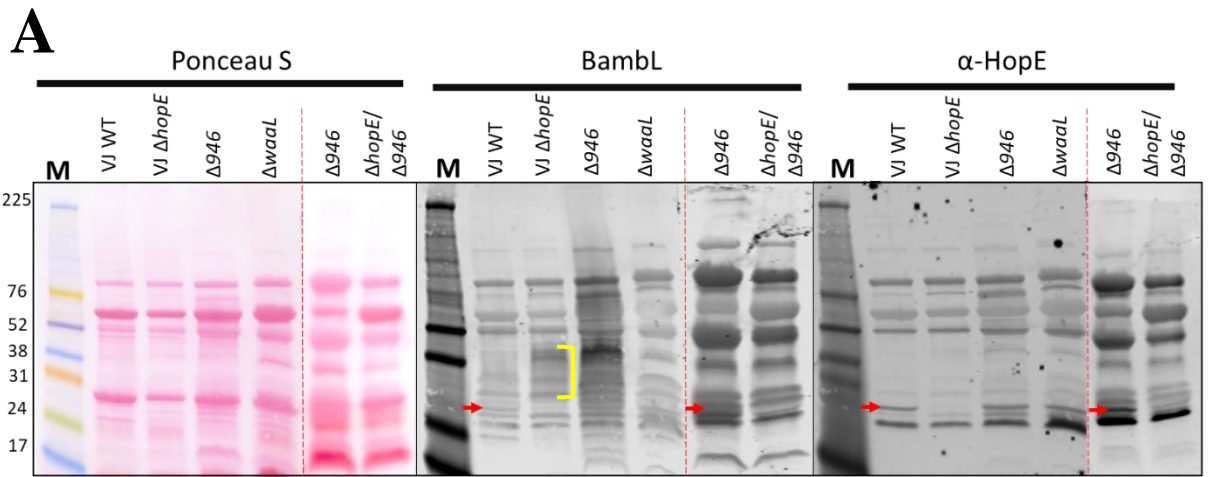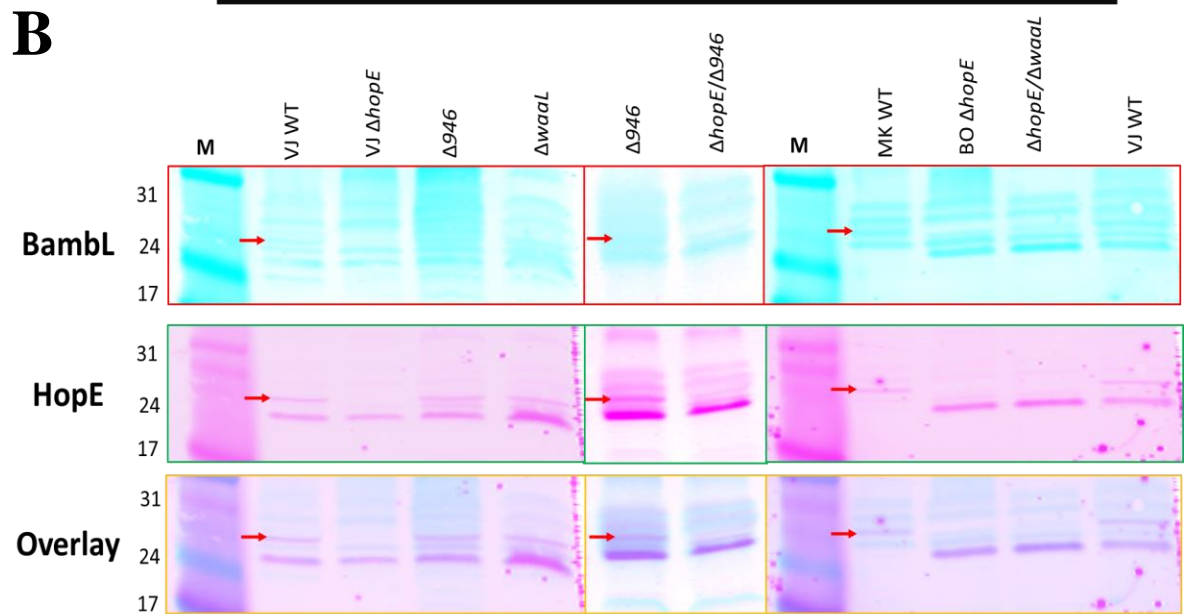
Figure 17. Ponceau S staining and Western blotting with BambL to investigate HopE glycosylation.

A) Western blot of OM preparations detected with BambL and anti-HopE antibodies on BioRad precast gradient gels (4-20%). Anti-HopE antibodies were used to re-probe the same membrane that had been incubated with BambL. Ponceau S stained membranes are shown on the left to visualize proteins. The red dashed lines indicate that the Δ*hopE* and Δ*hopE*/Δ*946* mutants shown together were run on different gels at a later date to the rest of the blot. Alignments were performed based on the molecular weight marker locations and overlaying blots. Sometimes, non-specifically reacting protein bands on both blots are also aligned. B) Enhanced view of the two blots. The blots were inverted to obtain the pink and blue colours using Photoshop in order to better visualize the bands when they are overlayed on top of each other. The red arrow indicates the location of the HopE band. The legend at the bottom matches the colour of each outlined box to its respective antibody/lectin. M = molecular weight markers.
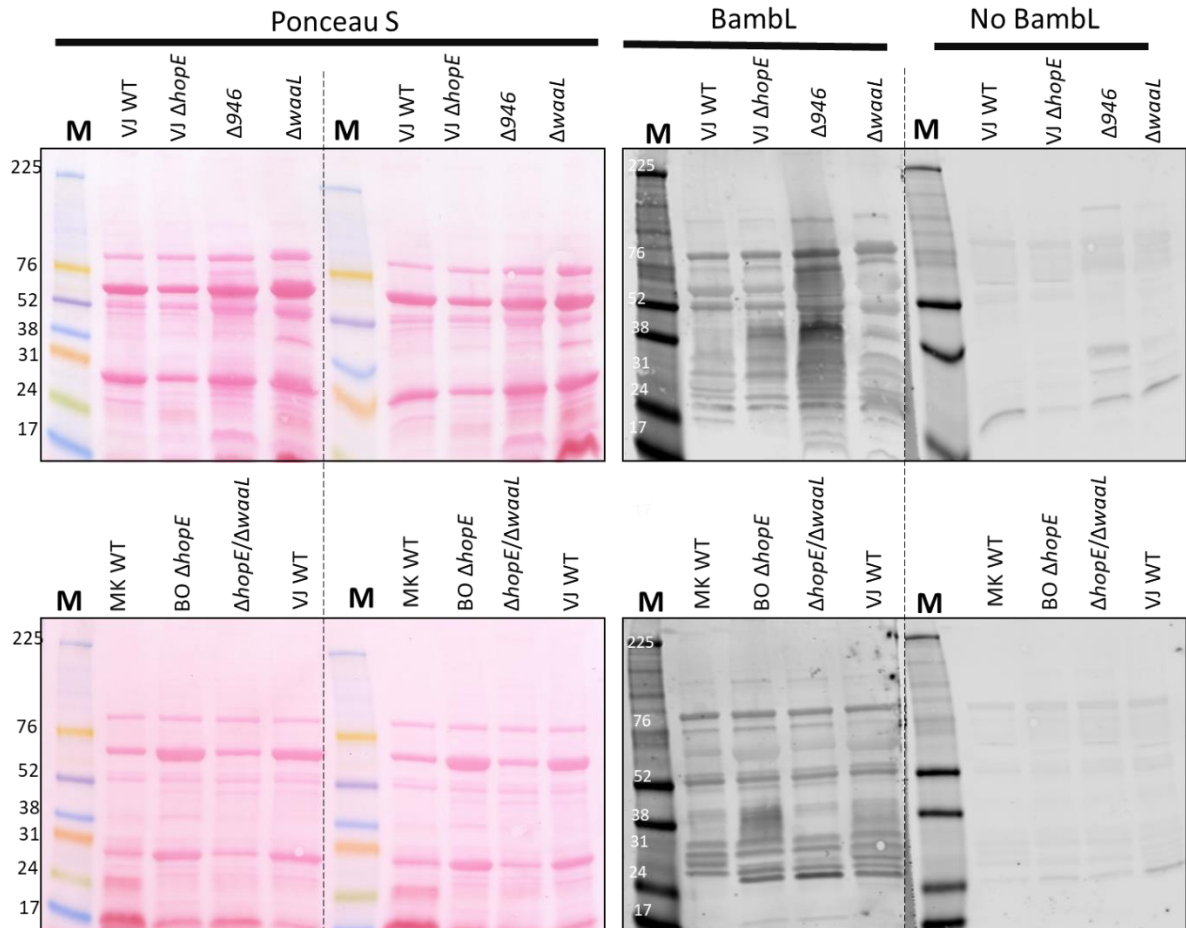
Figure 18. Ponceau S staining and Western blotting to detect non-specific binding by BambL lectin.

Western blot of OM samples with BambL and streptavidin on gradient gels (4-20%). Ponceau S stained membranes are shown on the left to visualize proteins. The "No BambL" portion of the membranes were generated to visualize non-specific binding of fluorescently labelled streptavidin. M = molecular weight markers.

3.5   Immunoprecipitation of HopE to obtain target protein

Rationale:

To reduce non-specific binding of antibodies to non-HopE proteins and LPS and to gain further evidence for/against the putative glycosylation of HopE, we aimed to isolate the HopE protein and perform targeted Western blotting (anti-Lewis Y and anti-HopE) without any interfering proteins or LPS. BambL Western blotting was also performed to determine the possibility of HopE being glycosylated by another fucosylated glycan.

Results:

Initially, the OM of VJ WT was lysed twice with the detergent Triton X-100; the first time with 0.2% Triton X-100 and the second time with 1% Triton X-100. The first lysate was then diluted by half to achieve an overall concentration of 0.1% Triton X-100 while the second lysate was diluted ten-fold before a sample was taken for gel analysis. These dilutions were performed to ensure that the concentration of the detergent did not affect downstream applications such as binding the lysate sample to the protein G-antibody mix.

The first lysate was incubated with the protein G-antibody mix because the concentration of HopE within the first lysate was more concentrated. As it was unclear how well the lysing with Triton X-100 would be in releasing HopE, the leftover insoluble unlysed portion of the OM preparations was also kept and run on the 12% SDS PAGE gel. The anti-HopE blot in Figure 19 shows that because HopE did not bind well to the protein G-antibody linked beads, it eluted in the unbound and wash steps. The protein that did elute in the elution step was roughly 50-55 kDa and is likely the heavy chain of the IgG antibody. However, it did appear that there were less non-HopE proteins being pulled down during this assay. There was not as many proteins reacting non-specifically to anti-HopE antibodies and less non-HopE reactivity in the Ponceau S stain as compared to the control lanes with OM samples of VJ WT and VJ Δ*hopE*. Thus, the blots are

cleaner than the other Western blots done without this process and our goal for performing this experiment was a success.

After blotting with the anti-HopE antibody, to determine the possibility of Lewis Y glycosylation, the membrane was re-probed with anti-Lewis Y (Figure 19). As the anti-Lewis Y blot indicates, there is no reactivity to the HopE band. This provides further confirmation that HopE is not glycosylated with Lewis Y.
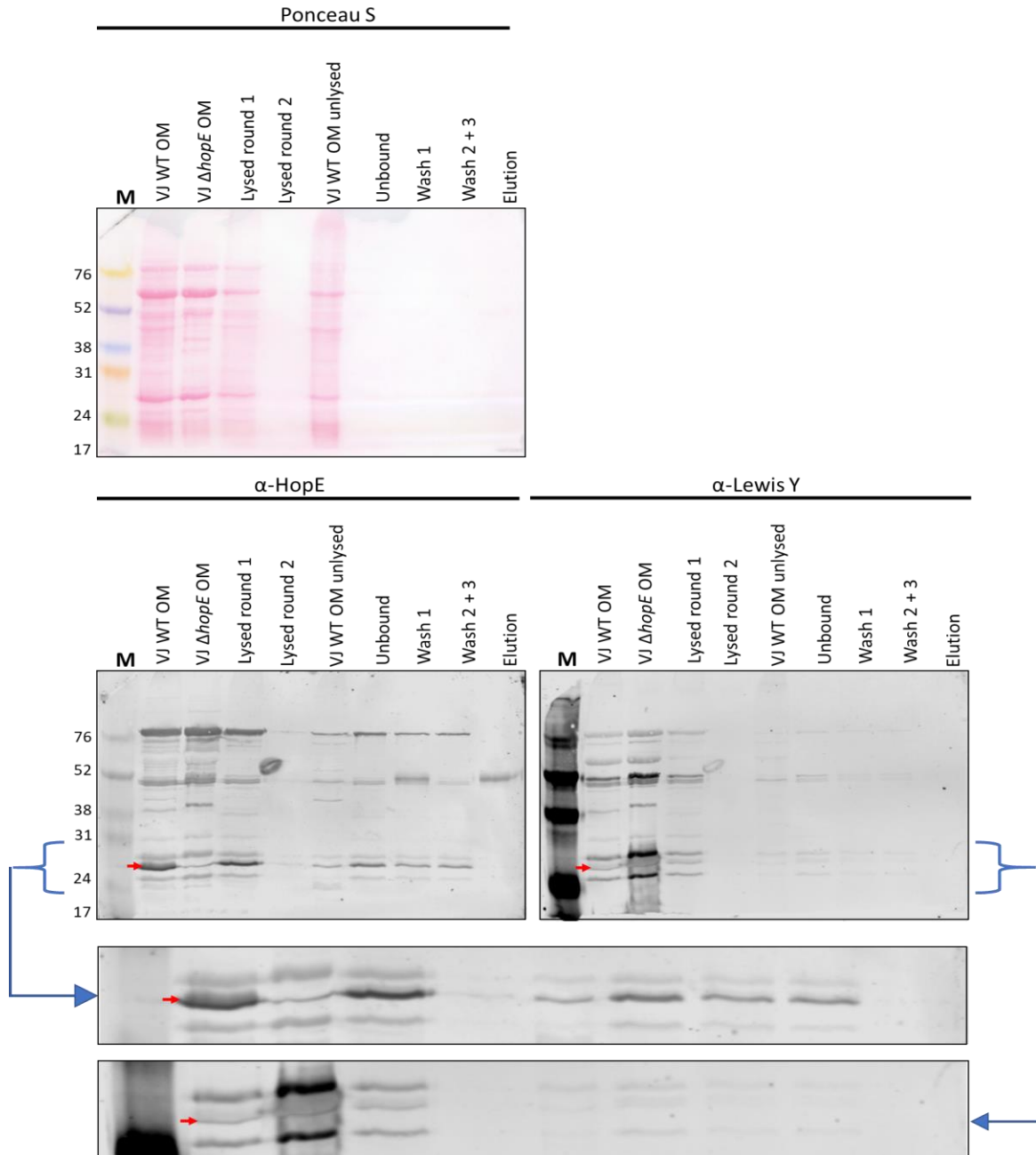
Figure 19. Immunoprecipitation of HopE results with Ponceau S, anti-HopE, and anti-Lewis Y detection.

After the immunoprecipitation attempt to elute HopE protein, all fractions of the immunoprecipitation assay were run on 12% SDS PAGE gels. Proceeding the Ponceau S staining and probing with anti-HopE, the same membrane was then re-probed with anti-Lewis Y. The red arrow indicates the location of HopE. Under the larger blots, the area of interest has been enhanced for easier visualization. M = molecular weight markers.

BambL Western blotting was also performed and compared to the anti-Lewis Y and anti-HopE blots (Figure 20). When the BambL and anti-HopE blots are examined together, the HopE band appears to be reacting to BambL. This is quite evident when viewing the OM control lanes for VJ WT and VJ Δ*hopE*; the HopE band clearly reacts to BambL in the WT while the lack of HopE expression in VJ Δ*hopE* also results in the lack of BambL reactivity in that area. This is significant considering that both samples were loaded equally according to the Ponceau S stain. When comparing this to the unbound and wash lanes, the BambL reactivity of HopE, although fainter than in the VJ WT control, is visible. This provides further evidence to the idea that HopE is glycosylated by a non-Lewis Y glycan that is fucosylated. Thus, glycosylation of HopE could still be linked to the LPS pathway via the fucosyltransferases that would be involved in generating this fucosylated glycan.
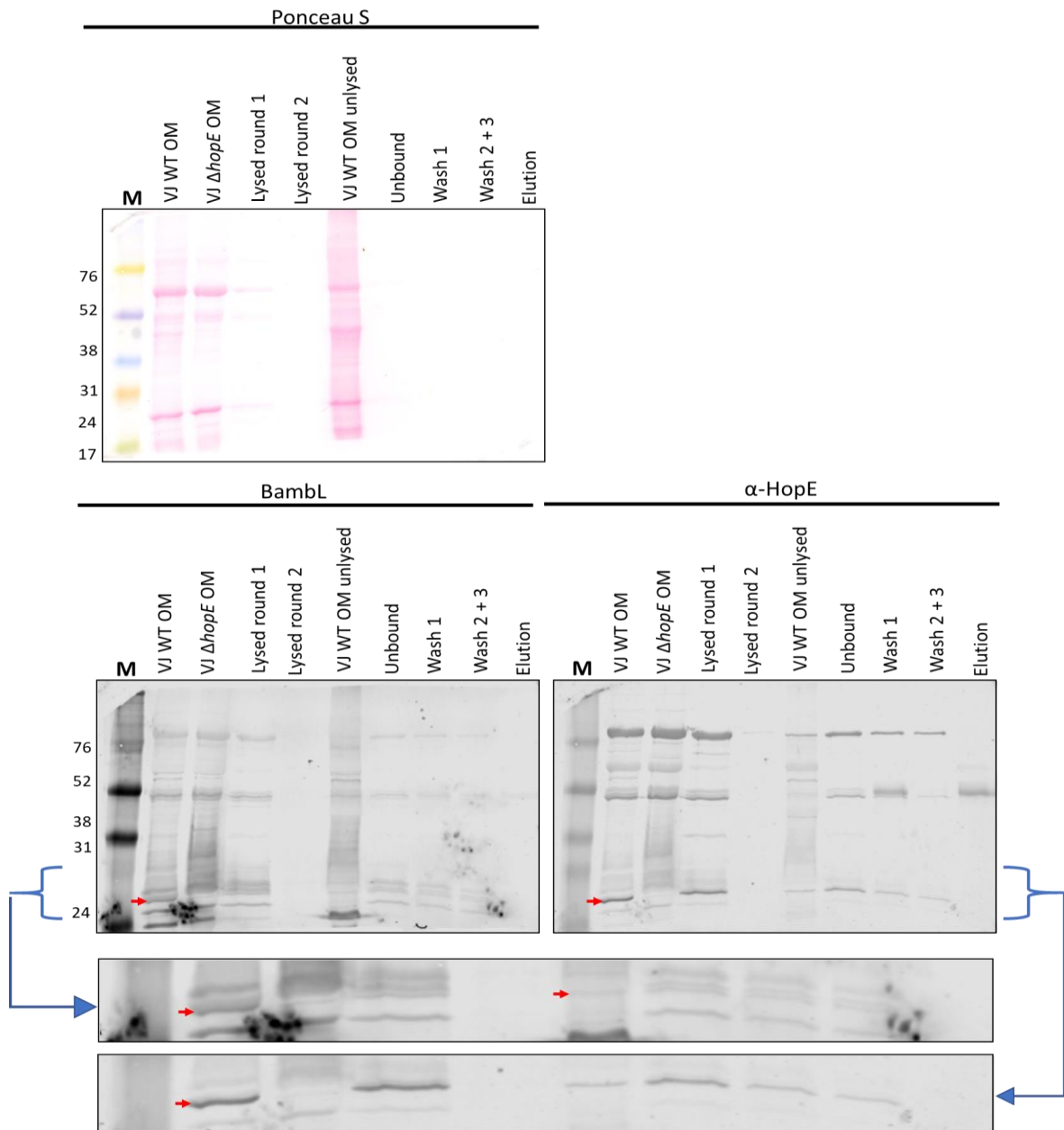
Figure 20. Immunoprecipitation of HopE results with Ponceau S, anti-HopE, and BambL detection.

After the immunoprecipitation attempt to elute HopE protein, all fractions of the immunoprecipitation assay were run on 12% SDS PAGE gels. Proceeding the Ponceau S staining and probing with BambL, the same membrane was then re-probed with anti-HopE. The red arrow indicates the location of HopE. Under the larger blots, the area of interest has been enhanced for easier visualization. M = molecular weight markers.

3.6 Testing HopE's role in antibiotic susceptibility/resistance via antibiotic sensitivity assays

Rationale:

Etest strips and disk diffusion methods were utilized to discover significant phenotypes amongst the Δ*hopE* mutants when compared to the WTs, Δ*waaL* (in the case of Δ*hopE*/Δ*waaL*) or Δ*946* (in the case of Δ*hopE*/Δ*946*). Performing both assays would help solidify any phenotypic variations we see between strains, as the results should be complementary to each other.

Results:

Table 4 shows the three different antibiotics that were used in this thesis. All three antibiotics are of different classes, have differing sizes and function via different mechanisms of action. This allowed us to observe the effect of HopE when subjected to antibiotics with varying attributes.
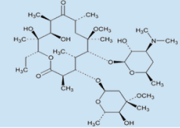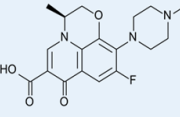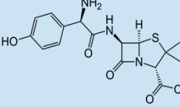
The levofloxacin Etest results demonstrate that VJ Δ*hopE* performs similarly to the WTs; removal of HopE sustains the same phenotype as VJ WT. Additionally, removal of HopE in the Δ*waaL* mutant maintains the Δ*waaL* phenotype in the Δ*hopE*/Δ*waaL* mutant and removing HopE in the Δ*hopE*/Δ*946* mutant keeps the Δ*946* phenotype (Table 5). Therefore, eliminating the porin HopE does not affect the minimum inhibitory concentration (MIC) compared with the original strains indicating that HopE does not play a role in levofloxacin susceptibility.

When observing the results in the amoxicillin Etest, all strains have the same MIC values except Δ*waaL* and Δ*hopE*/Δ*waaL*, with these two having the same lower MIC (Table 5). Thus, HopE does not influence the susceptibility of *H. pylori* to amoxicillin, similarly to the levofloxacin results. Overall, there is no significant difference between the strains, as CLSI standards dictate that significance is noted only if MICs are 4-fold dilutions apart.

The Δ*hopE* mutants within the disk diffusion assay (Figure 21) did not elicit a significant difference compared to the WTs, or the other background strains (Δ*waaL* and Δ*946*) in which the Δ*hopE*/Δ*waaL* and Δ*hopE*/Δ*946* mutants were made. This further indicates that the HopE porin likely does not play a role in antibiotic susceptibility. However, knocking out the HP0946 protein did result in greater susceptibility to clarithromycin in the disk diffusion assay, in a similar level of susceptibility as the Δ*waaL* and the Δ*hopE*/Δ*waaL* mutants.

With the loss of the full LPS barrier (specifically the O-antigen) against antibiotics for the mutants Δ*waaL* and Δ*hopE*/Δ*waaL*, this explains their increased susceptibility to antibiotics. However, this explanation can not be applied to Δ*946*, as the strain still produces what appears to be the full LPS O-antigen as evidenced by the anti-Lewis Y and BambL blots. An alternative explanation is yet to be discovered. It would be interesting to learn more about this protein in the future.

Table 4. Characteristics of antibiotics used for assessing antibiotic sensitivity.

Antibiotic Name	Class	Structure	Molecular Weight	Mechanism of Action	Bacteriostatic or Bactericidal
Clarithromycin (hydrophobic)	Macrolide		747.96 g/mol	inhibits protein synthesis; binds to 23S rRNA of the 50S ribosomal subunit	Bactericidal
Levofloxacin (lipophilic)	Fluoroquinolone		361.37 g/mol	inhibits DNA gyrase and prevents replication of DNA	Bactericidal
Amoxicillin (hydrophilic)	β-lactam		365.40 g/mol	inhibits cell wall synthesis	Bactericidal

The antibiotics used within this thesis are separated into several features. They all vary significantly in most characteristics.

Table 5. Results of the levofloxacin and amoxicillin Etest.

Strain	Levofloxacin MIC	Amoxicillin MIC
VJ WT	1.0	0.03
VJ ΔhopE	1.0	0.03
MK WT	0.5 − 1.0	0.03
BO ΔhopE	0.5	0.015 − 0.03
Δ946	0.5	0.03
ΔhopE/Δ946 Clone 6	0.25 − 0.5	0.03
ΔhopE/Δ946 Clone 7	0.25 − 0.5	0.03
ΔwaaL	0.5	0.015
ΔhopE/ΔwaaL	0.5	0.015

ΔhopE/ΔwaaL

This Etest strip test was conducted on three different days with *H. pylori* strains grown separately ($N = 3$). Cells were plated at a density of $OD_{600} = 0.5$. The brackets indicate strains that are apparently isogenic and can be compared. The MIC values that are in a range indicate that the strain varied in their response to the antibiotic once in the three replicates that were performed.
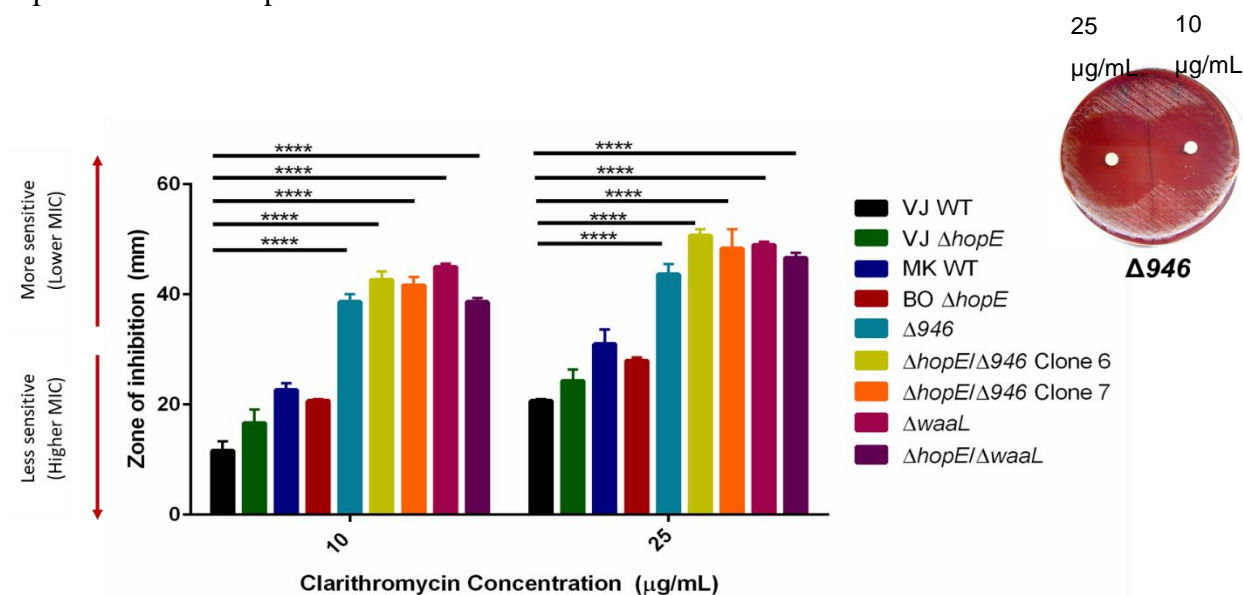
Figure 21. Results of the clarithromycin disk diffusion assay.

The disk diffusion assay was completed three times ($N = 3$), one technical replicate per each biological replicate, plated at a density of $OD_{600} = 0.5$. Mean ± SEM. Two-way ANOVA with Sidak's multiple comparison test, **** $P < 0.0001$.

3.7 Identifying a strategy for HopE complementation in Δ*hopE* mutant

Rationale:

Since the BambL reactivity seen in HopE is lost when HopE expression is eliminated in the Δ*hopE* mutant, this is a phenotype that can now be verified via complementation. The best method to date for performing complementation in *H. pylori* is through chromosomal integration using suicide plasmids. While making the plan to perform complementation, it was noticed that the suicide plasmids available in the lab containing the full HopE gene had the same antibiotic selection cassette downstream of HopE as the Δ*hopE* mutants (which were generated by disrupting the gene with a CAT cassette). This is because they were originally created for integration of the glycosylation point mutants of HopE in a WT strain. Thus, the antibiotic selection cassette would have to be swapped to a kanamycin selection cassette in order to correctly screen for transformants that had successfully incorporated the full *hopE* gene. However, swapping the plasmids for a kanamycin cassette was more time consuming and did not fit into the timeline of the project, thus it was not possible to complete this complementation in the remaining time.

Instead of performing the full complementation, we tested if the HopE plasmid complementation constructs obtained from previous lab mates would express the HopE protein once transformed into the VJ WT strain. The lab has produced two plasmids containing the full *hopE* gene. One is plasmid pMK35 from Maryam Khodai-Kalaki (MK) that contains no His-tag but has a CAT cassette while the other is from Brandon Oickle (BO) and contains a CAT cassette and a His-tag attached to the *hopE* gene. To note, neither plasmid constructs contain a promoter region in front of the *hopE* gene. Both are promoter-less genes that, once recombined in the chromosome in the *hopE* locus, should allow expression of HopE from its endogenous promoter as per design.

Both plasmids were transformed separately into the VJ WT strain in an effort to confirm that one of these constructs can be successfully incorporated into VJ WT and produce functional HopE protein. The production and location of the HopE protein would

be assessed by Western blotting with anti-HopE and anti-His using the OM samples of the two clones. If HopE is successfully expressed and observed in the Western blots, then the process of swapping the CAT cassette for the kanamycin cassette and completing the complementation can be undertaken in the future.

Result:

Transformation of the *hopE* genes followed by the CAT cassette with or without the His tag was successful (Figure 22). Two clones were chosen for downstream analysis, pMK35 706-His-less clone #1 and BO 706-His-CAT clone #5. The OMs of both clones were extracted, and Western blotting was performed.
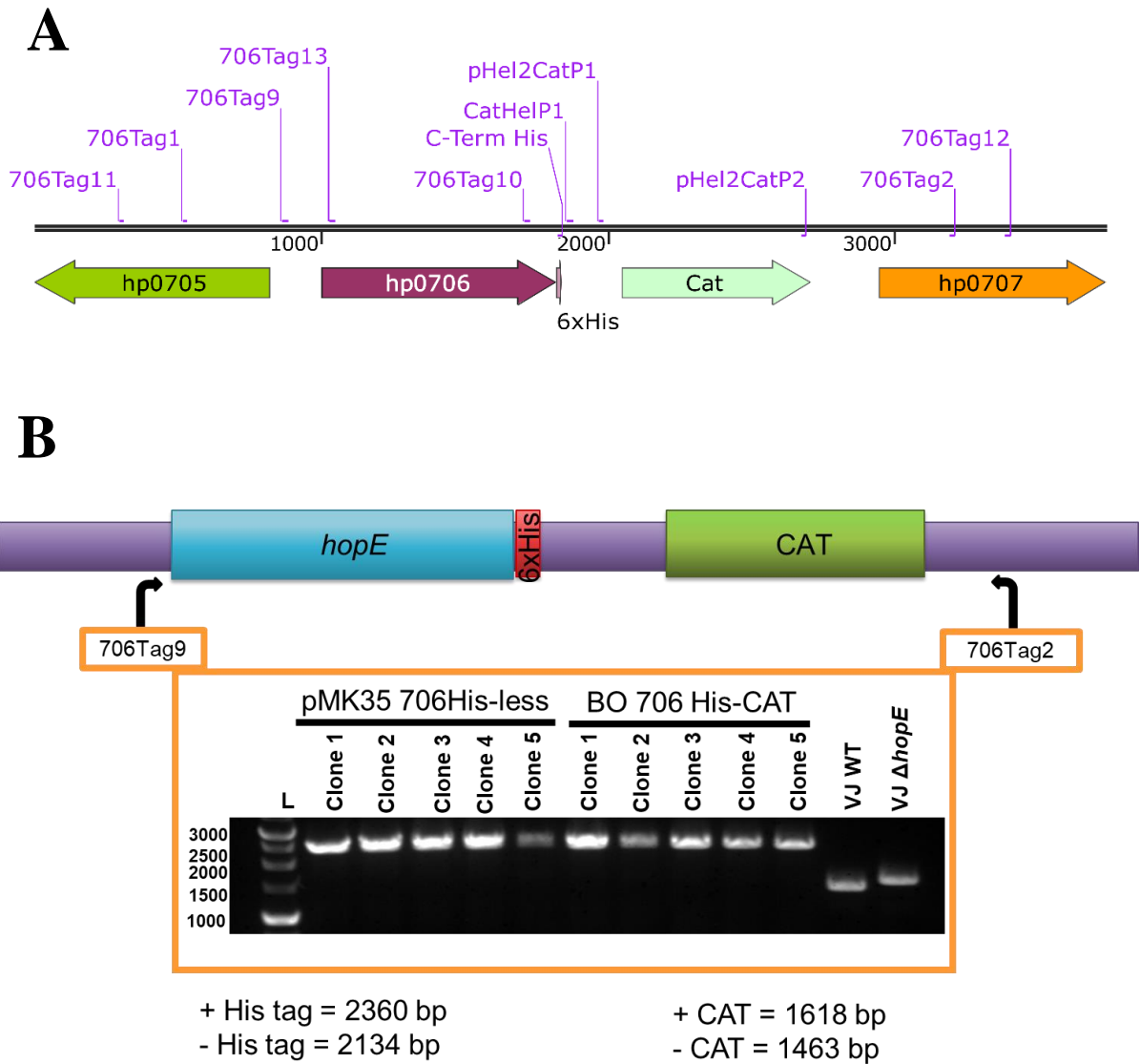
Figure 22. Generation of the *hopE* + CAT strains in VJ WT.
A) The *hopE*-His-CAT integration sequence showing the location of each possible primer available to use for PCR analysis. B) The location of the primers used to check the integration of the correct sequence is shown in the schematic above the gel result. Presence of the chloramphenical (CAT) resistance cassette and absence/presence of the His tag was verified by the increase in product size. HopE = HP0706. L = molecular weight standards.

Analysis of the new OM sample preparations of pMK35 706-His-less and BO 706-His-CAT by Western blot using anti-HopE antibodies show that background signal is observed in the lanes for these samples at a level similar to the Δ*hopE* mutant (Figure 23). As these plasmid constructs were transformed into VJ WT which has full HopE protein expression, shown on the Western blot in Figure 18, this absence of HopE expression indicates that the sequence of interest integrated into the correct location and subsequently eliminated the existing HopE expression. Through sequence analysis of the PCR product amplified using primers that span both upstream and downstream of the region containing the *hopE* and CAT genes (706Tag2 and 706Tag9), the sequence of *hopE* and the CAT cassette appear normal with no disruptions in their genes. However, the next step in this project would be to use primers that are located outside the recombination region and lie within the chromosomal DNA, such as 706Tag11 and 706Tag12. The resulting sequencing of these PCR products would provide information about the genes upstream and downstream of the recombination junction and whether they were affected in some that could give a reason for the loss of HopE.
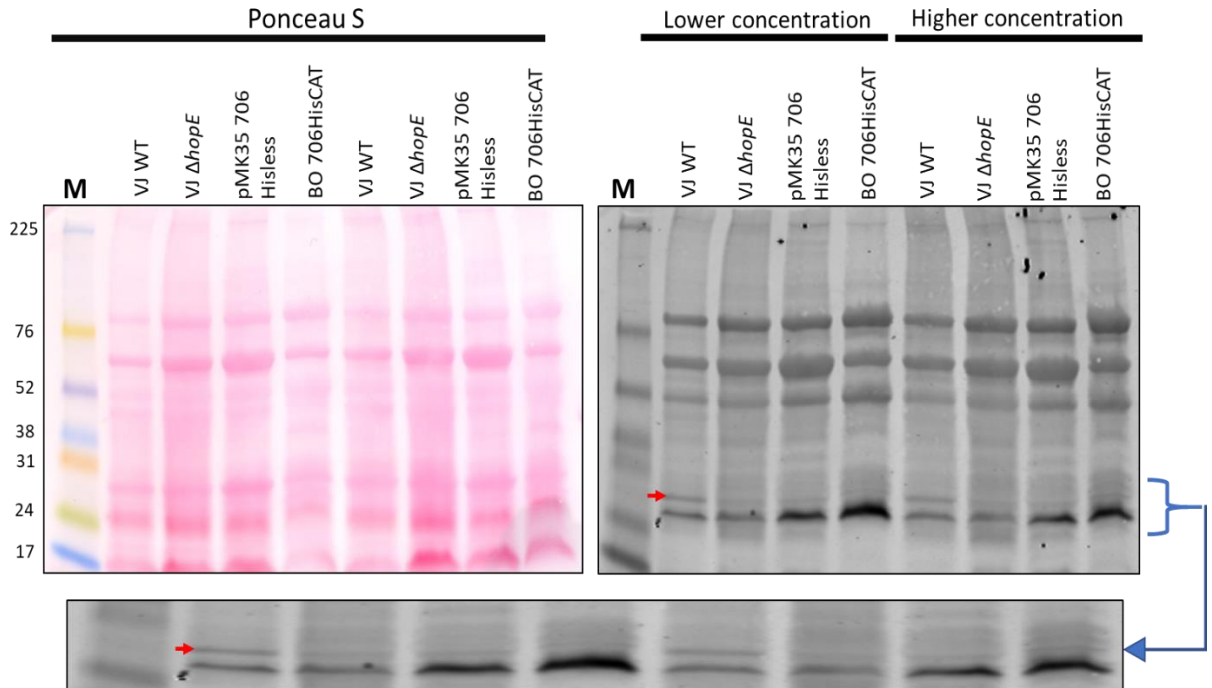
Figure 23. Analysis of HopE expression with Ponceau S staining anti-HopE Western blotting.

Western blot of OM samples run on 4-20% precast gradient gels. Ponceau S stain on the right. OM samples were loaded onto the gel in two concentrations, the lower and higher one. Loadings for each sample was defined by previous analysis with Coomassie staining after OM samples were prepared. The red arrow indicates the location of HopE. The enhanced section of interest in the blot is shown below. M = molecular weight markers.

Chapter 4: Discussion

4   Discussion

4.1   New anti-HopE antibodies successfully detect the HopE protein

Prior to the onset of my research into HopE glycosylation, there were no commercially available anti-HopE antibodies. My predecessors who had worked on this project had established the possibility that HopE might be glycosylated by Lewis Y using MS analysis and Western blotting. To connect the Lewis Y reactivity to HopE, custom-made anti-HopE antibodies were ordered using a predicted extracellular peptide of HopE with the amino acid sequence of GYKKFFQFKSLDMTS.

After obtaining the sera of two HopE immunized rabbits and determining the final ELISA results, rabbit #2's antibody sera was used as it had the higher antibody titer (Figure 6). However, there were several bleeds that were obtained during different timepoints within the immunization schedule of the rabbits. Thus, determining which bleed to use for successful detection of HopE was the priority. Using a step-wise gel with decreasing acrylamide concentration and extracting the outer membrane (OM) of the WT and *hopE* knockout strains using differential solubilization with N-laurylsarcosine, it was observed that all bleeds efficiently detected HopE. Using the Western blot (Figure 6) and the ELISA titer data, the final (fourth) bleed of rabbit #2 was utilized at a concentration of 1/200 for future experiments.

The use of the step-wise gels, while appropriate for ascertaining the working anti-HopE antibody concentration as seen in Figure 7, was not efficient at resolving the HopE protein from other proteins/LPS bands that were reacting to Lewis Y and co-localizing to the same area as HopE. After multiple attempts to further resolve HopE from non-HopE Lewis Y-reactive proteins/LPS bands in these step-wise gels, it was decided that gradient gels may be the best solution for this recurring issue. Thus, precast gradient gels (4-20%) were purchased from BioRad. In Figure 7, the results obtained by the precast gels can be seen. The gradient gels could effectively condense and resolve the proteins and LPS into distinct bands, allowing for greater protein comparability between lanes within the same blot and within different blots. The use of commercially produced gradient gels also

allowed for highly reproducible and standardized blots, with proteins running to the same location every single time.

4.2   HopE glycosylation in *Helicobacter pylori*

With the discovery of a ~31 kb protein that reacted to anti-Lewis Y in our lab, MS analysis suggested that the protein was possibly HopE. However, with the acquisition of working anti-HopE antibodies, this idea could be verified for certain. To aid in the identification of HopE as a glycoprotein, the double knockout mutant Δ*hopE/*Δ*waaL* was successfully generated to observe the HopE protein without interfering LPS structures in both Western blots and functional assays. Nevertheless, it was important to consider that this Δ*hopE/*Δ*waaL* mutant does have the potential to abrogate glycosylation if WaaL serves as the oligosaccharide transferase (OST). If WaaL was not the OST, the synthesis of O-units would still be preserved and could be transferred onto HopE by the true OST, such as HP0946.

From examining the results of the anti-HopE and anti-Lewis Y blots (Figure 14), it is evident that the reactivity of the Lewis Y antibodies in the area of HopE does not change in response to the loss of the HopE protein in the Δ*hopE* mutants (in WT or in the Δ*waaL* background strains). This is likely because HopE is not glycosylated by Lewis Y. However, one caveat to mention is that as there appears to be a strongly reacting band to Lewis Y in the same area as where the HopE localizes, and this might mask the loss of Lewis Y signal if HopE was glycosylated with Lewis Y. It is likely, according to MS data, that HopE would only have one unit of Lewis Y motif, thus it might not be easily detected by the Lewis Y antibody so its loss in the Δ*hopE* mutants would not be visible when compared to the other proteins/LPS also reacting in that area. Objective 2 of the hypothesis was to determine if the HP0946 protein is the Lewis oligosaccharide transferase (OST) for HopE glycosylation. These series of blots determined that HP0946 is not the OST for HopE Lewis Y glycosylation. This is evidenced by the lack of any changes to the Lewis Y reactivity in the HopE area for the Δ*946* mutant.

Conversely, the BambL blots (Figure 17), that detect fucosylated epitopes which include Lewis Y but also non-Lewis Y epitopes, showed the opposite. When HopE expression was eliminated, it appeared that BambL reactivity was also absent. Thus, there is evidence that HopE may be glycosylated by a non-Lewis Y glycan. However, like the anti-Lewis Y blot illustrated, the Δ*946* mutant still had BambL reactivity in the HopE area, meaning HP0946 is not an OST for the HopE protein. With this result, it is important to try to elucidate both the identity of the non-Lewis Y glycan and the identity of the OST responsible for transferring the glycan to HopE.

To note, Figures 15, 16, and 18 show the results of testing for non-specificity from the secondary antibody. The results illustrate that although all blots, especially the anti-HopE blot (Figure 14), have multiple bands, these bands are not due to non-specific binding by the secondary antibody. The multiple bands seen on Figures 14 and 17 when using both primary and secondary antibodies/lectin are likely due to the antibody/lectin reacting to proteins/LPS that contain the epitopes of interest.

Additionally, eliminating HP0946 expression causes the generation of higher molecular weight bands that are reactive to both Lewis Y and BambL. This is evidenced when comparing the Proteinase K treated samples in the anti-Lewis Y and BambL Western blot in Figure 13 to the blots in Figure 14 and 17. Currently, there are a couple unknown aspects of this discovery, such as whether these bands are LPS or proteins and the function of HP0946. However, since HP0946 is localized to the inner membrane, it is entirely possible that eliminating this protein may indeed affect the LPS synthesis pathway as most of the proteins involved in that pathway are also found within the inner membrane. Again, a complete answer for this phenotype is yet forthcoming.

The discovery of an outer membrane protein with an unknown fucose-containing glycan signifies the importance of molecular mimicry in *H. pylori*. Although it is not Lewis Y, as a fucose-containing glycan it may still be Lewis X, Lewis a or Lewis b, which are human blood group antigens[73].

4.3   Variations in LPS pattern for different *H. pylori* strains

To achieve further observation of the LPS pattern in the working strains, PK treated OM samples were visualized using the silver staining method. Treating the OM samples with PK should effectively digest the protein content and leave the LPS molecules intact. In the silver stain of Figure 12, there is a discrepancy in the LPS pattern when comparing the WTs and Δ*waaL* mutant and Δ*hopE/ΔwaaL* double knockout mutant to the Δ*hopE* and Δ*946* mutants. The WTs and Δ*waaL* mutant and Δ*hopE/ΔwaaL* double knockout mutant do not have the higher silver-reactive bands (~31 – 40 kDa, indicated by a green bracket) that are seen in the Δ*hopE* and Δ*946* mutants. Initially, it was assumed that this was evidence for a variation of the LPS between the WTs and the Δ*hopE* and Δ*946* mutants. The results of the *waaL* and Δ*hopE/ΔwaaL* mutants are as expected since these strains do not have the O-antigen ligase therefore they would not have a full LPS pattern. Additionally, it was confirmed that the lanes containing OM PK-treated samples from the Δ*hopE* and Δ*946* mutants do have higher silver-reactive bands that are likely LPS and not proteins. This was verified by the concurrently performed Coomassie stain, which does not show those bands, indicating they were not protein bands that were PK resistant.

However, the WT strains also had less lipid-A core concentrations in the Figure 12 silver stain, implying that although every effort was taken to aim for equal loading, the WT samples may not have been loaded as strongly as the other strains. Thus, another silver stain was conducted with freshly extracted WT OM samples and the new OM samples of Δ*hopE*/Δ*946* mutant. As Figure 13 clearly demonstrates, despite our best efforts to ensure equal loading in Figure 12, there was a loading issue for the WTs that resulted in the low visibility of the higher LPS molecules via silver stain. In fact, the best way to visualize the higher LPS molecules was to cut out that area and re-stain with silver.

This variation in O-antigen expression between each OM extraction could also play a role in influencing each individual antibiotic assay, making it very important to have replicates of each assay, regardless of how reproducible the tests reportedly are (such as the Etest). To summarize, both silver staining and Coomassie results indicate

that the LPS molecules seen in the 31-40 kDa range are present in all the strains and do not change depending on a specific mutant.

4.4 Immunoprecipitation of HopE to identify HopE glycosylation

To definitively determine the presence/absence of HopE glycosylation, production of cleaner Western blots without interfering proteins or LPS was attempted. Therefore, purification of HopE through immunoprecipitation was required. However, the protein HopE is part of the insoluble outer membrane section of HP, rendering the outcome of conventional immunoprecipitation assays to purify HopE uncertain.

In an attempt to make the insoluble OM portion more soluble and subsequently release the HopE protein into the soluble supernatant, the OM sample of VJ WT was subjected to lysing via Triton X-100, a non-ionic detergent. As the effectiveness of this attempt remained unclear, the OM sample was lysed twice, first with 0.2% Triton X-100 and diluted by half in buffer solution and the second time with 1% Triton X-100 and diluted ten-fold. However, only the first lysis was subjected to immunoprecipitation since it would have the higher concentration of soluble HopE protein.

After running all the immunoprecipitation fractions on an anti-HopE Western blot (Figure 19), it was evident that although the blot was cleaner and contained less proteins, the HopE protein had not bound well to the protein G-antibody linked beads. The reason for this is likely due to the pH of the buffer containing dimethyl pimelimidate (DMP), the cross-linking reagent, being below pH 8. If the pH of the solution falls below 8, or rises above 9, the cross-linking efficiency of DMP is greatly reduced[74]. However, the pH of the solution was 7.42 in response to the isoelectric point of HopE being 8.86, since the efficient functioning of the sodium phosphate buffer requires its pH to be at least 0.5 pH units away from the isoelectric point of the HopE protein. Thus, the DMP was not effectively cross-linking the antibody to the protein G beads, resulting in a weak bond that could easily dissociate and elute early the antibody and the HopE protein. One future

direction to obtain better immunoprecipitation results would be to increase the pH of the buffer solution to around pH 8.3; this should allow DMP to work effectively. Regardless of this low cross-linking efficiency, immunoprecipitation was still a success as it reduced non-HopE protein and allowed for more targeted Western blotting assays to be performed.

After confirming the presence of the HopE proteins in the immunoprecipitation fractions using anti-HopE antibodies, the membrane was re-blotted with anti-Lewis Y to determine the potential for Lewis Y glycosylation. As in previous anti-Lewis Y Western blots shown in this thesis, the cleaner Western blot showed that Lewis Y was not reactive to HopE (Figure 19). This is the best proof that HopE is not glycosylated by Lewis Y. However, the reactivity of BambL to HopE seen in Figure 17 indicates that while HopE may not contain the Lewis Y glycan, it does appear to be glycosylated by a non-Lewis Y glycan that contains fucose. Previous research conducted by other labs has shown that HP NCTC 11637 also contains H-type O-antigens[75] and BambL has shown to bind preferentially to H-type glycan compared to Lewis Y[76]. Thus, it is possible that the glycan in question is an H-type, which only contains the fucose on the terminating end of the O-antigen.

The putative glycosylation of HopE aligns with porin glycosylation in previous literature. Currently, there are only two well-established porin glycoproteins: *C. jejuni*'s major outer membrane protein (MOMP)[63] and *P. aeruginosa*'s OprD[64]. However, among the three porins, glycosylation occurs using differing glycans, whereby the MOMP is glycosylated with one galactose and three GalNAc residues, OprD contains 3 sialylated N-glycans and 2 sialylated O-glycans, and HopE is glycosylated with a fucose-containing glycan. Importantly, the glycosylation of MOMP was observed to occur at T_{268}, which is in a surface exposed loop as was found in HopE. In this thesis, the role of HopE and its glycosylation in antibiotic resistance was studied, as porin OprD plays a role in antibiotic susceptibility[64]. As evidence shows that HopE is likely glycosylated, one future direction (once complementation has established HopE as a glycoprotein) could be to study the role of HopE's glycosylation in other processes such as those studied in MOMP.

Glycosylation of this MOMP porin indicated a correlation to promoting bacteria-to-bacteria binding, biofilm formation, and adhesion to Caco-2 cells.

4.5 The HopE porin likely does not play a role in antibiotic susceptibility

Previous research into other porins have implicated porins as a passage for antibiotics into the cell[15,77], such as *Escherichia coli*'s OmpC[78], *Acinetobacter baumannii*'s OmpA[79], and *Vibrio cholerae*'s OmpU[80]. Additionally, it was also shown that sialylation of the porin OprD of *Pseudomonas aeruginosa* resulted in decreased uptake of β-lactam antibiotics through this porin[64]. Thus, the possibility that HopE and its putative glycosylation play a role in antibiotic resistance was explored via the use of several antibiotics and multiple antibiotic sensitivity assays.

Table 3 lists the various types of antibiotics used, each with a different mechanism of action to target various processes within the bacterial cell. These three specific antibiotics were also chosen due to their clinical relevance, as they are all used in triple and quadruple therapy treatments to combat HP infection[10]. Using these antibiotics, different antibiotic sensitivity assays were employed, including spot plating, gradient agar plate method, E-tests and disk diffusion assays. Each assay was meant to complement one another; however, not all the assays lead to reproducible results.

The spot plating method is a long exposure test conducted by incorporating the test antibiotic into blood agar media and observing the growth of the bacteria. As we did not know which specific concentration of each antibiotic would be effective at differentiating the strains, three different concentrations for all antibiotics used were tested (data not shown). To note, the strains were grown on solid media instead of a broth because HP does not grow well in broth. HP simply survives, which is not adequate for antibiotic sensitivity testing as several antibiotics target peptidoglycan growth and protein synthesis, so the bacteria need to be actively growing. Once the proper optical density was achieved, the cultures were serially diluted 10-fold for 8 dilutions and spot-plated on the antibiotic-incorporated plates. Two strains were tested on one plate with one antibiotic at a specific concentration. Thus, a single strain was tested on three

concentrations of one antibiotic, plus a control containing just the background antibiotics usually used and no test antibiotic. Once the bacterial colonies had grown well enough to count them, the CFU/mL was calculated and compared among strains. Results from multiple trials of this assay proved to be inconsistent and the colonies were hard to count accurately. This assay was also not as high throughput as was required to test the large number of strains that were studied within this thesis; thus, the spot plating method was set aside.

As another method of testing antibiotic sensitivity, the strains were grown on antibiotic gradients via the gradient agar plate method (data not shown). In this assay, the plates are manually created and the initial antibiotic used was clarithromycin, as it was the most promising antibiotic that gave differences between the strains in the spot plating method. The plates are laid out on a slant and the agar containing the test antibiotic is poured into the plate. After this layer cooled down, that plates were placed back on level surface and agar with only background antibiotics were poured. Once cooled, the plates were flipped upside down and the antibiotics began to diffuse, thus establishing a gradient of antibiotic concentration. According to literature, as antibiotics can diffuse in the plates, the plates should be used not too long after the 12 hour mark[81]. The HP strains are then spread via sterile glass beads on the gradient plates and the control plate (no gradient, no test antibiotic) and incubated for 16 hours. Results of this method showed that there were no discernible changes in growth density across the gradient plates. It was decided that this method may not be the best assay for a slow growing organism, as the antibiotic gradient may be lost before it can successfully affect HP growth, which would especially be a problem if the antibiotic was bacteriostatic. This assay was abandoned after two trials.

Following the failure of the spot plating and gradient agar method, Etest strips were purchased for levofloxacin and amoxicillin. Etest strips are considered the gold standard for testing the response of bacteria to antibiotics in clinical laboratories. The strips also generate highly reproducible results, are easy to use, and are high throughput. At the time, commercial strips for clarithromycin were unavailable so the disk diffusion assay was implemented for this antibiotic.

Considering the results of the levofloxacin Etest, most strains did not react significantly different to each other, including the WTs and VJ Δ*hopE* (Table 5). This provides evidence that eliminating HopE expression does not cause an increase in susceptibility or resistance. This was further proven by the double knockout mutant Δ*hopE*/Δ*waaL*, which was initially created to compare against the Δ*hopE* and Δ*waaL* mutants. As the LPS O-antigen is lost in this double knockout, this loss should allow the antibiotics to have clearer access to the HopE porin without the steric hindrance provided by the LPS molecules on the outer membrane. However, it appeared that any increase in susceptibility that this double knockout mutant exhibits could be attributed to the phenotype caused by the elimination of the O-antigen ligase WaaL as can be seen in the single Δ*waaL*. Furthermore, contrasting the longer BambL- and Lewis Y-reactive LPS pattern seen in the VJ Δ*hopE* mutant (Figures 14 and 17) with the shorter one observed in VJ WT also indicated that this variation in LPS does not affect the way these two strains interact with levofloxacin, which aligns with the silver stain gel (Figure 13) that shows no variation in the LPS. These results are also mirrored in the amoxicillin Etest results.

The purpose of the Δ*hopE*/Δ*946* mutant was to eliminate HopE expression in a strain that had LPS matching the LPS of the Δ*hopE* mutant. This was effective, and the LPS pattern of the Δ*hopE*/Δ*946* mutant remained the same as its respective single mutants. Through the successful generation of the Δ*hopE*/Δ*946* mutants, there is further evidence that eliminating HopE does not change the susceptibility of the Δ*hopE*/Δ*946* mutant to levofloxacin or amoxicillin compared to the single Δ*946* mutant. This same outcome was also seen in the antibiotic sensitivity results for Δ*hopE*/Δ*waaL* in that eliminating HopE didn't affect how Δ*hopE*/Δ*waaL* reacted to the antibiotic compared to the Δ*waaL* mutant.

To overcome the lack of clarithromycin Etest strips, this assay was performed by adding two different concentrations of clarithromycin to separate homemade disks and placing the disks on a lawn of bacteria, similar to the Etest. This method, while cheaper than the Etest strips, was slightly more time consuming and required some trial and error to get the right working concentrations of antibiotics to obtain readable zones of inhibition. However, the results of this test were very reproducible, and the method

allowed for higher throughput as multiple disks of different antibiotic concentrations could be placed on a single plate with the bacterial lawn. As Figure 21 demonstrates, when comparing the WTs to the Δ*946*¸ *ΔwaaL* and double knockout mutants, the results of this assay closely resembled those of the Etest disks and were more highly visual. Again, Δ*hopE* mutants did not vary from the WTs, similar to the Etests.

Collectively, all these antibiotic tests show that eliminating HopE does not cause a significant difference when matching the mutant to its isogenic strain (be it the WT strain, Δ*waaL* mutant, or Δ*946* mutant) for either levofloxacin, amoxicillin or clarithromycin. HopE does not play a role in antibiotic susceptibility. Interestingly, the results of the disk diffusion method showed that eliminating HP0946 increased the susceptibility of the Δ*946* strain to clarithromycin; the results were significantly different compared to the WT strains and similar to the Δ*waaL* and the Δ*hopE*/Δ*waaL* mutants which are lacking the full LPS structure. As seen in the anti-Lewis Y and BambL blots, the Δ*946* mutant has its full LPS therefore an alternate explanation must be discovered. Very little is known about this protein, which has been annotated as a sodium-proton antiporter but never confirmed. One hypothesis is that perhaps HP0946 is involved in either preventing entry of antibiotics across the inner membrane or may be involved in extruding antibiotics back to the periplasm.

4.6 Working towards a functional complementation strategy to restore *hopE* expression in the Δ*hopE* mutant

Through the elimination of HopE expression, it was discovered that WT strains contain a BambL-reactive band in the HopE protein region that is lost in the *hopE* knockout mutants, implicating the existence of HopE as a fucose-containing glycoprotein. To verify that this is a robust phenotype, complementation would be the next step of this project. However, due to the suicide plasmids with full HopE constructs containing the same selection cassette as the *hopE* mutants, swapping the selection cassette to kanamycin was beyond the timeline of my project. Thus, to ensure that the plasmids containing the full *hopE* gene would successfully integrate into the knockout mutant and allow expression of the HopE protein, these HopE promoter-less plasmids pMK35 706-His-less and BO 706-His-CAT were separately transformed successfully

into VJ WT. The purpose of the histidine tag within the clone created by BO was in an attempt to tag and purify the HopE protein as purification of proteins using affinity chromatography with nickel targeting the His tag had been proven to provide high protein yields and purity of over 95%[82]. This tag was added to the C-terminus of the protein to prevent its removal when the N-terminal signal sequences of the protein is cleaved during transport into the periplasm[83]. Subsequent nickel affinity chromatography did not detect His tagged HopE in the outer membrane fractions. It was assumed that this method for identifying His tagged HopE proteins was ineffective given the circumstances or that the His tag may prevent proper folding and OM localization of HopE. However, at the time of the creation of this His tagged HopE, there were no anti-HopE antibodies to confirm that His tagging might have altered HopE protein expression itself.

Two of the resulting clones from each set of transformations were analyzed via PCR using primers that spanned the length of the gene sequence of interest (Figure 22), 706Tag9 annealed within the integrating construct while 706Tag2 annealed to the chromosomal DNA downstream of the region of recombination. The sequencing data indicated that both the *hopE* gene and the CAT cassette gene had successfully incorporated into the VJ WT genome without mutations and that the sequence inserted into the correct area. Therefore, the outer membranes were extracted from one clone from each transformation and subjected to anti-HopE Western blotting.

Comparing the WT, Δ*hopE,* pMK35 706-His-less and BO 706-His-CAT samples to each other indicated that incorporation of the new *hopE* gene sequence into the VJ WT eliminated the expression of HopE entirely, similar to the Δ*hopE* mutant. This elimination also indirectly confirmed that the plasmids had recombined correctly and inserted the sequence into the right area. One of the reasons for this lack of HopE protein expression could be due to the His tag attached to the HopE protein. Perhaps the His tag prevented proper folding of the HopE protein, resulting in the protein being degraded and prevented from being exported to the outer membrane. Conversely, the pMK35 706-His-less clone should not have a functional His tag and sequence analysis showed that the His sequence is still there with a stop codon placed before it to prevent its translation. Lack of HopE expression in this clone indicated that either the stop codon and His sequence still

resulted in disrupting HopE expression, perhaps because of mRNA instability, or something else unrelated to the His tag DNA sequence was the cause of the loss of protein expression. It may be possible that integration of this sequence causes gene disruptions either upstream or downstream of the integration area.

4.7 Summary and future directions

To re-iterate, the objectives of this project were:

1) Optimize the detection of HopE using anti-HopE antibodies to determine whether HopE is glycosylated, via anti-Lewis Western blotting.

2) Investigate the role of the Lewis oligosaccharide transferase HP0946 in potential HopE glycosylation and determine its connection to LPS synthesis.

3) Elucidate the functional impact of HopE and its putative Lewis glycosylation in regard to antibiotic resistance/susceptibility.

To highlight objective 1, this study demonstrated the presence of HopE as a novel glycoprotein that is glycosylated by a currently unknown glycan containing fucose. This was done in part through the successful optimization of the anti-HopE antibodies, regardless of the serum's propensity to cross-react with non-HopE OM proteins with similar epitopes to the porin. Although initially it was thought that the glycan was Lewis Y, after comparing the anti-Lewis Y blots with anti-HopE, it became clear that this was not the case. Through the use of the BambL lectin, it was determined that the glycan did contain a fucose (like Lewis Y) but was another as yet unidentified glycan.

As a result, a future direction of this study is to further characterize this HopE glycoprotein and determine the glycan with which it is glycosylated. The next step in this characterization would be to develop strategies to specifically purify for HopE and other glycoprotein candidates that react to BambL. In this case, affinity for the BambL lectins can be utilized to purify for glycoprotein candidates from the unmodified proteins. For this method, BambL lectin could be coupled to a matrix containing sepharose. Subsequently, the BambL lectin can be used to purify the fucose-modified glycoproteins

(including HopE) via affinity chromatography. Once purified by this method, the glycoprotein candidates can be sent for MS analysis for identification of the proteins and the glycan itself.

Nevertheless, the results of this thesis also indicate that contrary to our hypothesis for objective 2, HP0946 is not the OST that glycosylates HopE as the HopE band is still present and BambL-reactive in the Δ*946* mutant during Western blotting. Furthermore, this work also eliminates the possibility that the O-antigen ligase may play the role of OST for HopE as the same HopE band is BambL-reactive in the Δ*waaL* mutant. We showed that HopE is glycosylated with a fucose-containing glycan, which does not eliminate non-Lewis Y antigens (such as Lewis X, a, or b) which were presumed to be exclusively associated with the LPS. Thus, it is still possible that glycosylation in HP is linked to the LPS synthesis pathway. Further studies are needed to determine the precise relationship between the two processes, whereby the impetus lies in identifying the OST for this glycosylation of HopE.

Moreover, the deletion of HP0946 expression also causes the increased generation of LPS/protein bands reactive to both Lewis Y and BambL. As an inner membrane protein, the elimination of HP0946 would likely also affect the LPS synthesis pathway as most enzymes related to this pathway also exist in the inner membrane.

To ensure that lack of BambL-reactive glycoprotein in the Δ*hopE* mutants and the antibiotic susceptibility in the Δ*946* mutant are true phenotypes, a future direction would be to facilitate the successful complementation of both mutants. The complementation of HopE was initiated in this thesis with two suicide plasmids, one containing the HopE with a His tag and the other without it. However, clones from both transformations showed no expression of HopE when subjected to an anti-HopE blot. A future direction for this method would be to use primers that span entirely outside the recombination area and within the chromosomal DNA, such as 706Tag11 and 706Tag12. Sequencing the resulting PCR product could indicate if the genes upstream and downstream of the recombination junction were affected in some way, providing a reason for the loss of HopE production. Additionally, another attempt can be conducted on transforming VJ

WT using a suicide plasmid without the DNA sequence for the His tag at all. The results of this attempt would determine if the His tag DNA sequence was the reason for the loss of the protein expression or if the act of recombination resulted in an unforeseen mutation elsewhere in the chromosome that affected HopE production.

By successfully creating a plasmid that will subsequently be transformed into the recipient strain Δ*hopE* and express HopE, this would be the crucial step in working towards complementation of HopE. Once this step is completed and the correct antibiotic cassettes are being utilized, the VJ Δ*hopE* mutant can be complemented and the glycosylation of HopE can be confirmed. Similarly, a plasmid vector containing the full *HP0946* gene construct should also be created and transformed into the Δ*946* recipient strain for verification of the LPS variation and antibiotic susceptibility phenotypes.

Currently, the functional impact of neither HopE nor its putative glycosylation has been elucidated, as objective 3 had suggested. Antibiotic testing with three different substances of varying characteristics (levofloxacin, amoxicillin and clarithromycin) all present the same results, demonstrating that HopE does not play a discernible role in antibiotic susceptibility. However, a novel discovery indicates that HP0946 may have a link to antibiotic sensitivity since eliminating HP0946 causes an increase in clarithromycin susceptibility for the Δ*946* and Δ*hopE*/Δ*946* mutants. One explanation put forth for this involved HP0946 facilitating the prevention of entry of antibiotics across the inner membrane or extruding the antibiotic back to the periplasm. Therefore, the future direction for this aspect of the project would be to complement the Δ*946* mutant and test with the same antibiotics to ensure this phenotype is a result of the loss of HP0946. Once this is established, a further examination into the mechanism of HP0946 in relation to antibiotics must follow.

In summary, we showed that HopE is glycosylated with a fucose-containing glycan, and it may have a link to LPS synthesis which will be corroborated once the complementation has been completed. HP0946 was observed to not be the OST of interest, and neither was WaaL. We also show that HP0946's elimination appears to result in a generation of more LPS or glycoproteins that are BambL and Lewis Y

reactive. HP0946 also may be linked to antibiotic interaction and may increase susceptibility to clarithromycin when its protein expression is lost. These discoveries provide new insight into the mechanisms of *H. pylori* and the tools it uses to evade the host immune response and develop immunity to current antibiotic treatments.

References

1.   Dunn, B. E., Cohen, H. & Blaser, M. J. *Helicobacter pylori*. **10,** 720–741 (1997).

2.   Marshall, B. & Warren, J. R. Unidentified curved bacilli in the stomach of patients with gastritis and peptic ulceration. *Lancet* **323,** 1311–1315 (1984).

3.   Ahmed, N. 23 years of the discovery of *Helicobacter pylori*: Is the debate over? *Ann. Clin. Microbiol. Antimicrob.* (2005). doi:10.1186/1476-0711-4-17

4.   Marshall, B. J., Armstrong, J. A., McGechie, D. B. & Glancy, R. J. Attempt to fulfil Koch's postulates for pyloric *Campylobacter*. *Med. J. Aust.* **142,** 436–9 (1985).

5.   Kusters, J. G., Van Vliet, A. H. M. & Kuipers, E. J. Pathogenesis of *Helicobacter pylori* infection. *Clinical Microbiology Reviews* (2006). doi:10.1128/CMR.00054-05

6.   Hooi, J. K. Y. *et al.* Global prevalence of *Helicobacter pylori* infection: systematic review and meta-analysis. *Gastroenterology* **153,** 420–429 (2017).

7.   Kuipers, E. J., Thijs, J. C. & Festen, H. P. The prevalence of *Helicobacter pylori* in peptic ulcer disease. *Aliment. Pharmacol. Ther.* **9 Suppl 2,** 59–69 (1995).

8.   Uemura, N., Okamoto, S. & Yamamoto, Soichiro, et al. *Helicobacter pylori* infection and the development of gastric cancer. *N. Engl. J. Med.* **345,** 784–789 (2001).

9.   World Cancer Research Fund International. Stomach cancer statistics | World Cancer Research Fund International. Available at: https://www.wcrf.org/int/cancer-facts-figures/data-specific-cancers/stomach-cancer-statistics. (Accessed: 31st May 2018)

10.   Testerman, T. L. & Morris, J. Beyond the stomach: an updated view of *Helicobacter pylori* pathogenesis, diagnosis, and treatment. *World J. Gastroenterol.* **20,** 12781–808 (2014).

11.   Pellicano, R., Zagari, R. M., Zhang, S., Saracco, G. M. & Moss, S. F. Pharmacological considerations and step-by-step proposal for the treatment of *Helicobacter pylori* infection in the year 2018. *Minerva Gastroenterol. Dietol.* (2018). doi:10.23736/S1121-421X.18.02492-3

12.   Mégraud, F. Recent advances in clinical practice in *Helicobacter pylori* antibiotic resistance: prevalence, importance and advances in testing. *Gut* **53,** 1374–1384 (2004).

13.   WHO | WHO publishes list of bacteria for which new antibiotics are urgently needed. *WHO* (2017).

14.   Lerouge, I. & Vanderleyden, J. O-antigen structural variation: mechanisms and possible roles in animal/plant–microbe interactions. *FEMS Microbiol. Rev.* **26,** (2002).

15. Delcour, A. H. Outer membrane permeability and antibiotic resistance. *Biochim. Biophys. Acta* **1794,** 808–16 (2009).

16. Chow, J. C., Young, D. W. & Golenbock, D T, et al. Toll-like receptor-4 mediates lipopolysaccharide-induced signal transduction. *J. Biol. Chem.* **274,** 10689–92 (1999).

17. Stead, C. M., Zhao, J., Raetz, C. R. H. & Trent, M. S. Removal of the outer Kdo from *Helicobacter pylori* lipopolysaccharide and its impact on the bacterial surface. *Mol. Microbiol.* **78,** 837–852 (2010).

18. Stead, C. M., Beasley, A., Cotter, R. J. & Trent, M. S. Deciphering the unusual acylation pattern of *Helicobacter pylori* lipid A. *J. Bacteriol.* **190,** 7012–21 (2008).

19. Yamaoka Y. *Helicobacter pylori: Molecular Genetics and Cellular Biology - Google Books*.

20. Appelmelk, B. J., Simoons-Smit, I. & Negrini, R, et al. Potential role of molecular mimicry between *Helicobacter pylori* lipopolysaccharide and host Lewis blood group antigens in autoimmunity. *Infect. Immun.* **64,** 2031–40 (1996).

21. Cullen, T. W., Giles, D. K. & Wolf, Lindsey N., et al. *Helicobacter pylori* versus the host: remodeling of the bacterial outer membrane is required for survival in the gastric mucosa. *PLoS Pathog.* **7,** e1002454 (2011).

22. Li, H., Liao, T. & Debowski, Aleksandra W, et al. Lipopolysaccharide structure and biosynthesis in *Helicobacter pylori*. *Helicobacter* (2016). doi:10.1111/hel.12301

23. Hug, I., Couturier, M. R. & Rooker, Michelle M., et al. *Helicobacter pylori* lipopolysaccharide Is synthesized via a novel pathway with an evolutionary connection to protein N-glycosylation. *PLoS Pathog.* **6,** e1000819 (2010).

24. Nilsson, C. *et al.* An enzymatic ruler modulates Lewis antigen glycosylation of *Helicobacter pylori* LPS during persistent infection. *Proc. Natl. Acad. Sci. U. S. A.* **103,** 2863–8 (2006).

25. Moran, A. P., Knirel, Y. A. & Senchenkova, S. N., et al. Phenotypic variation in molecular mimicry between *Helicobacter pylori* lipopolysaccharides and human gastric epithelial cell surface glycoforms: acid-induced phase variation in Lewis(x) and Lewis(y) expression by *H. pylori* lipopolysaccharides. *J. Biol. Chem.* **277,** 5785–5795 (2002).

26. Alaimo, C., Catrein, I. & Morf, Laura, et al. Two distinct but interchangeable mechanisms for flipping of lipid-linked oligosaccharides. *EMBO J.* **25,** 967–76 (2006).

27. Wirth, H. P., Yang, M., Karita, M. & Blaser, M. J. Expression of the human cell surface glycoconjugates Lewis x and Lewis y by *Helicobacter pylori* isolates is related to cagA status. *Infect. Immun.* **64,** 4598–605 (1996).

28. Kobayashi, M., Lee, H., Nakayama, J. & Fukuda, M. Carbohydrate-dependent defense mechanisms against *Helicobacter pylori* infection. *Curr. Drug Metab.* **10,** 29–40 (2009).

29.   Monteiro, M. a *et al.* Simultaneous expression of type 1 and type 2 Lewis blood group antigens by *Helicobacter pylori* lipopolysaccharides. Molecular mimicry between *H. pylori* lipopolysaccharides and human gastric epithelial cell surface glycoforms. *J. Biol. Chem.* **273,** 11533–11543 (1998).

30.   Logan, R. P., Berg, D. E. & Tomb, JF, et al. Genetic diversity of *Helicobacter pylori*. *Lancet* **348,** 1462–3 (1996).

31.   Appelmelk, B. J. & Vandenbrouck-Grauls, C. M. J. E. Phase variation in *Helicobacter pylori* lipopolysaccharide. *Infect. Immun.* (2003). doi:10.1016/B978-012194851-1/50032-9

32.   Alm, R. A., Bina, J. & Andrews, B M., et al. Comparative genomics of *Helicobacter pylori*: analysis of the outer membrane protein families. *Infect. Immun.* **68,** 4155–68 (2000).

33.   Doig, P., Exner, M. M., Hancock, R. E. & Trust, T. J. Isolation and characterization of a conserved porin protein from *Helicobacter pylori*. *J. Bacteriol.* **177,** 5447–52 (1995).

34.   Ilver, D., Arnqvist, A. & Ogren, J., et al. *Helicobacter pylori* adhesin binding fucosylated histo-blood group antigens revealed by retagging. *Science (80-.).* **279,** 373–7 (1998).

35.   Bina, J., Bains, M. & Hancock, R. E. Functional expression in *Escherichia coli* and membrane topology of porin HopE, a member of a large family of conserved proteins in *Helicobacter pylori*. *J. Bacteriol.* **182,** 2370–5 (2000).

36.   Skouloubris, S., Thiberge, J. M., Labigne, A. & De Reuse, H. The *Helicobacter pylori UreI protein is not involved in urease activity but is essential for bacterial survival in vivo. Infect. Immun.* **66,** 4517–21 (1998).

37.   Weeks, D. L., Eskandari, S., Scott, D. R. & Sachs, G. A H+-gated urea channel: the link between *Helicobacter pylori* urease and gastric colonization. *Science* **287,** 482–5 (2000).

38.   Trainor, E. A., Horton, K. E., Savage, P. B., Testerman, T. L. & McGee, D. J. Role of the HefC Efflux Pump in *Helicobacter pylori* Cholesterol-Dependent Resistance to Ceragenins and Bile Salts. *Infect. Immun.* **79,** 88–97 (2011).

39.   Nothaft, H. & Szymanski, C. M. Protein glycosylation in bacteria: sweeter than ever. *Nat. Rev. Microbiol.* **8,** 765–778 (2010).

40.   Walski, T., De Schutter, K., Van Damme, E. J. M. & Smagghe, G. Diversity and functions of protein glycosylation in insects. *Insect Biochem. Mol. Biol.* **83,** 21–34 (2017).

41.   Lis, H. & Sharon, N. Protein glycosylation. Structural and functional aspects. *Eur. J. Biochem.* **218,** 1–27 (1993).

42.   Medzihradszky, K. F. Characterization of site-specific N-glycosylation. *Methods Mol. Biol.* **446,** 293–316 (2008).

43.   Kowarik, M., Young, N. M. & Numao, Shin, et al. Definition of the bacterial N-

glycosylation site consensus sequence. *EMBO J.* **25,** 1957–66 (2006).

44. Fletcher, C. M., Coyne, M. J., Villa, O. F., Chatzidaki-Livanis, M. & Comstock, L. E. A general O-glycosylation system important to the physiology of a major human intestinal symbiont. *Cell* **137,** 321–331 (2009).

45. Hopf, P. S., Ford, R. S. & Zebian, N. et al. Protein glycosylation in *Helicobacter pylori*: beyond the flagellins? *PLoS One* **6,** e25722 (2011).

46. Apweiler, R., Hermjakob, H. & Sharon, N. On the frequency of protein glycosylation, as deduced from analysis of the SWISS-PROT database. *Biochim. Biophys. Acta* **1473,** 4–8 (1999).

47. Schiller, B., Hykollari, A., Yan, S., Paschinger, K. & Wilson, I. B. H. Complicated N-linked glycans in simple organisms. *Biol. Chem.* **393,** 661–73 (2012).

48. Gemmill, T. R. & Trimble, R. B. Overview of N- and O-linked oligosaccharide structures found in various yeast species. *Biochim. Biophys. Acta - Gen. Subj.* **1426,** 227–237 (1999).

49. Mescher, M. F. & Strominger, J. L. Purification and characterization of a prokaryotic glycoprotein from the cell envelope of *Halobacterium salinarium*. *J. Biol. Chem.* **251,** 2005–14 (1976).

50. Thibault, P. *et al.* Identification of the Carbohydrate Moieties and Glycosylation Motifs in *Campylobacter jejuni* Flagellin. *J. Biol. Chem.* **276,** 34862–34870 (2001).

51. Schirm, M., Soo, E. C. & Aubry, A J, et al. Structural, genetic and functional characterization of the flagellin glycosylation process in *Helicobacter pylori*. *Mol. Microbiol.* **48,** 1579–92 (2003).

52. Szymanski, C. M., Logan, S. M., Linton, D. & Wren, B. W. *Campylobacter*--a tale of two protein glycosylation systems. *Trends Microbiol.* **11,** 233–8 (2003).

53. Scott, N. E. *et al.* Simultaneous Glycan-Peptide Characterization Using Hydrophilic Interaction Chromatography and Parallel Fragmentation by CID, Higher Energy Collisional Dissociation, and Electron Transfer Dissociation MS Applied to the *N* -Linked Glycoproteome of *Campylobacter jejuni*. *Mol. Cell. Proteomics* **10,** M000031-MCP201 (2011).

54. Kelly, J. *et al.* Biosynthesis of the N-Linked glycan in *Campylobacter jejuni* and addition onto protein through block transfer. *J. Bacteriol.* **188,** 2427–2434 (2006).

55. Wacker, M. *et al.* N-Linked glycosylation in *Campylobacter jejuni* and its functional transfer into *E. coli*. *Science (80-.).* **298,** 1790–1793 (2002).

56. Hendrixson, D. R. & DiRita, V. J. Identification of *Campylobacter jejuni* genes involved in commensal colonization of the chick gastrointestinal tract. *Mol. Microbiol.* **52,** 471–484 (2004).

57. Szymanski, C. M., Burr, D. H. & Guerry, P. Campylobacter protein glycosylation affects host cell interactions. *Infect. Immun.* **70,** 2242–4 (2002).

58. Guerry, P. *Campylobacter* flagella: not just for motility. *Trends Microbiol.* **15,**

456–461 (2007).

59. Howard, S. L. *et al. Campylobacter jejuni* glycosylation island important in cell charge, legionaminic acid biosynthesis, and colonization of chickens. *Infect. Immun.* **77,** 2544–2556 (2009).

60. Zebian, N. *et al.* Comprehensive analysis of flagellin glycosylation in *Campylobacter jejuni* NCTC 11168 reveals incorporation of legionaminic acid and its importance for host colonization. *Glycobiology* **26,** 386–397 (2016).

61. Logan, S. M. Flagellar glycosylation - a new component of the motility repertoire? *Microbiology* **152,** 1249–1262 (2006).

62. Hug, I. & Feldman, M. F. Analogies and homologies in lipopolysaccharide and glycoprotein biosynthesis in bacteria. *Glycobiology* **21,** 138–151 (2011).

63. Mahdavi, J. *et al.* A novel O-linked glycan modulates *Campylobacter jejuni* major outer membrane protein-mediated adhesion to human histo-blood group antigens and chicken colonization. *Open Biol.* **4,** 130202 (2014).

64. Khatua, B., Vleet, J. Van, Choudhury, B. P., Chaudhry, R. & Mandal, C. Sialylation of outer membrane porin protein D: A mechanistic basis of antibiotic uptake in *Pseudomonas aeruginosa. Mol. Cell. Proteomics* **13,** 1412–1428 (2014).

65. Tabei, S. M. B., Hitchen, P. G. & Day-Williams, Michaela J, et al. An *Aeromonas caviae* genomic island is required for both O-antigen lipopolysaccharide biosynthesis and flagellin glycosylation. *J. Bacteriol.* **191,** 2851–63 (2009).

66. Merkx-Jacques, A., Obhi, R. K. & Bethune, G., et al. The *Helicobacter pylori* flaA1 and wbpB genes control lipopolysaccharide and flagellum synthesis and function. *J. Bacteriol.* **186,** 2253–65 (2004).

67. Miller, W. L., Matewish, M. J. & McNally, David J, et al. Flagellin glycosylation in *Pseudomonas aeruginosa* PAK requires the O-antigen biosynthesis enzyme WbpO. *J. Biol. Chem.* **283,** 3507–18 (2008).

68. Creuzenet, C. & Lam, J. S. Topological and functional characterization of WbpM, an inner membrane UDP-GlcNAc C6 dehydratase essential for lipopolysaccharide biosynthesis in *Pseudomonas aeruginosa. Mol. Microbiol.* **41,** 1295–1310 (2001).

69. Koenigs, M. B., Richardson, E. A. & Dube, D. H. Metabolic profiling of *Helicobacter pylori* glycosylation. *Mol. Biosyst.* **5,** 909–12 (2009).

70. Champasa, K., Longwell, S. A., Eldridge, A. M., Stemmler, E. A. & Dube, D. H. Targeted identification of glycosylated proteins in the gastric pathogen *Helicobacter pylori* (Hp). *Mol. Cell. Proteomics* **12,** 2568–86 (2013).

71. Fomsgaard, A., Freudenberg, M. A. & Galanos, C. Modification of the silver staining technique to detect lipopolysaccharide in polyacrylamide gels. *J. Clin. Microbiol.* **28,** 2627–31 (1990).

72. Tomb, J.-F. *et al.* The complete genome sequence of the gastric pathogen *Helicobacter pylori. Nature* **388,** 539–547 (1997).

73. Martins, L. C. *et al.* ABH and Lewis antigen distributions in blood, saliva and

gastric mucosa and *H. pylori* infection in gastric ulcer patients. *World J. Gastroenterol.* **12,** 1120–4 (2006).

74. Cross-linking antibodies to beads protocol | Abcam. Available at: http://www.abcam.com/protocols/cross-linking-antibodies-to-beads-protocol. (Accessed: 23rd June 2018)

75. Appelmelk, B. J. & Vandenbroucke-Grauls, C. M. J. E. *Lipopolysaccharide Lewis Antigens. Helicobacter pylori: Physiology and Genetics* (ASM Press, 2001).

76. Audfray, A. *et al.* Fucose-binding lectin from opportunistic pathogen *Burkholderia ambifaria* binds to both plant and human oligosaccharidic epitopes. *J. Biol. Chem.* **287,** 4335–47 (2012).

77. Fernández, L. & Hancock, R. E. W. Adaptive and mutational resistance: role of porins and efflux pumps in drug resistance. *Clin. Microbiol. Rev.* **25,** 661–81 (2012).

78. Jaffe, A., Chabbert, Y. A. & Semonin, O. Role of porin proteins OmpF and OmpC in the permeation of beta-lactams. *Antimicrob. Agents Chemother.* **22,** 942–8 (1982).

79. Iyer, R., Moussa, S. H., Durand-Réville, T. F., Tommasi, R. & Miller, A. *Acinetobacter baumannii* OmpA Is a Selective Antibiotic Permeant Porin. *ACS Infect. Dis.* **4,** 373–381 (2018).

80. Pagel, M. *et al.* Phenotypic characterization of pore mutants of the *Vibrio cholerae* porin OmpU. *J. Bacteriol.* **189,** 8593–600 (2007).

81. Yuqing, L. *et al.* SCIENCE CHINA Accurate assessment of antibiotic susceptibility and screening resistant strains of a bacterial population by linear gradient plate. **54,** 953–960 (2011).

82. Rudd, P. M. & Dwek, R. A. Glycosylation: Heterogeneity and the 3D Structure of Proteins. *Crit. Rev. Biochem. Mol. Biol.* **32,** 1–100 (1997).

83. Carlsson, F. *et al.* Signal sequence directs localized secretion of bacterial surface proteins. *Nature* **442,** 943–946 (2006).

Curriculum Vitae

Name: Keertika Yogendirarajah

Post-secondary Education and Degrees:

Western University
London, Ontario, Canada
2016 – 2018
MSc Candidate

University of Waterloo
Waterloo, Ontario, Canada
2011 – 2016
BSc Honours Biology Co-op, Psychology Minor

Honours and Awards:

Canadian Institute of Health Research (CIHR), 2017-2018
$17,500

Dr. F.W Luney Graduate Entrance Scholarship, 2016
Western University
$3000

Sandilands Family Entrance Scholarship, 2011
University of Waterloo
$1000

Queen Elizabeth II Aiming for the Top, 2011- 2016
University of Waterloo
$3000/year

President's Scholarship, 2011
University of Waterloo
$1000

Related Work Experience

Graduate Teaching Assistant
Western University
MicroImm 3500B Social and Biological Determinants of Disease
2017-2018

Undergraduate Teaching Assistant
BIOL 241L, Introduction to Applied Microbiology Lab
Jan – Apr 2016

Undergraduate Teaching Assistant
BIOL 444, Microorganisms and Disease Lab
Sept – Dec 2015

Student Research Assistant, Co-op
Department of Laboratory Medicine and Pathobiology
University of Toronto
Jan – Aug 2015

Undergraduate Teaching Assistant
BIOL 240L, Introduction to Microbiology
Sept – Dec 2014

Publications:

Williams-Dautovich, J, Yogendirarajah, K., dela Cruz, A., Tsai, R., Grynpas, M.D., Cummins, C.L. (2017). The CRH-transgenic Cushingoid mouse is a model of glucocorticoid-induced osteoporosis. J Bone Miner Res. Plus. DOI: 10.1002/jbm4.10009.

Williams-Dautovich, J, Yogendirarajah, K., dela Cruz, A., Patel, R., Tsai, R., Grynpas, M.D., Cummins, C.L. (2017). LXR antagonism modulates glucocorticoid- induced osteoclastogenesis but does not protect against osteoporosis in a Cushing's mouse model. (In preparation).

Poster Presentations:

Yogendirarajah, K., Creuzenet, C. (2018) Exploring the function of a novel porin in *Helicobacter pylori*. Presented at the Banff Conference on Infectious Diseases.

Yogendirarajah, K., Oberc A., Khodai-Kalaki, M., Zebian, N., Creuzenet C. (2018). Investigating the function of a novel porin in *Helicobacter pylori*. Presented at the London Health Research Day.

Yogendirarajah, K., Oberc A., Khodai-Kalaki, M., Zebian, N., Creuzenet C. (2017). Performing functional assays on the novel porin HopE in *Helicobacter pylori*. Presented at the Infection and Immunity Research Forum.

Yogendirarajah, K., Oberc A., Khodai-Kalaki, M., Zebian, N., Creuzenet C. (2017). Elucidating the function of a novel porin in *Helicobacter pylori*. Presented at the Canadian Society of Microbiologists Conference.

Yogendirarajah, K., Creuzenet C. (2017). Establishing a Western blot methodology to elucidate the glycosylation of HopE protein. Presented at the London Health Research Day.

Yogendirarajah, K., Williams-Dautovich, J., Cummins, C.L. and Grynpas, M.D. (2015). The role of LXR antagonism in glucocorticoid-induced osteoporosis using a Cushingoid mouse model.
Presented at the Lunenfeld-Tanenbaum Research Institute Summer Student Poster Presentation.